







RESEARCH

Open Access



A subset of gut leukocytes has telomerase-dependent “hyper-long” telomeres and require telomerase for function in zebrafish

Pam S. Ellis^{1†} , Raquel R. Martins^{1†} , Emily J. Thompson¹ , Asma Farhat¹ , Stephen A. Renshaw²  and Catarina M. Henriques^{1*} 

Abstract

Background: Telomerase, the enzyme capable of elongating telomeres, is usually restricted in human somatic cells, which contributes to progressive telomere shortening with cell-division and ageing. T and B-cells cells are somatic cells that can break this rule and can modulate telomerase expression in a homeostatic manner. Whereas it seems intuitive that an immune cell type that depends on regular proliferation outbursts for function may have evolved to modulate telomerase expression it is less obvious why others may also do so, as has been suggested for macrophages and neutrophils in some chronic inflammation disease settings. The gut has been highlighted as a key modulator of systemic ageing and is a key tissue where inflammation must be carefully controlled to prevent dysfunction. How telomerase may play a role in innate immune subtypes in the context of natural ageing in the gut, however, remains to be determined.

Results: Using the zebrafish model, we show that subsets of gut immune cells have telomerase-dependent “hyper-long” telomeres, which we identified as being predominantly macrophages and dendritics (*mpeg1.1⁺* and *cd45⁺mhcll⁺*). Notably, *mpeg1.1⁺* macrophages have much longer telomeres in the gut than in their haematopoietic tissue of origin, suggesting that there is modulation of telomerase in these cells, in the gut. Moreover, we show that a subset of gut *mpeg1.1⁺* cells express telomerase (*tert*) in young WT zebrafish, but that the relative proportion of these cells decreases with ageing. Importantly, this is accompanied by telomere shortening and DNA damage responses with ageing and a telomerase-dependent decrease in expression of autophagy and immune activation markers. Finally, these telomerase-dependent molecular alterations are accompanied by impaired phagocytosis of *E. coli* and increased gut permeability in vivo.

[†]Pam S. Ellis and Raquel R. Martins contributed equally to this work.

*Correspondence: c.m.henriques@sheffield.ac.uk

¹The Bateson Centre, MRC-Arthritis Research UK Centre for Integrated Research Into Musculoskeletal Ageing and Department of Oncology and Metabolism, Healthy Lifespan Institute, University of Sheffield Medical School, Sheffield, UK

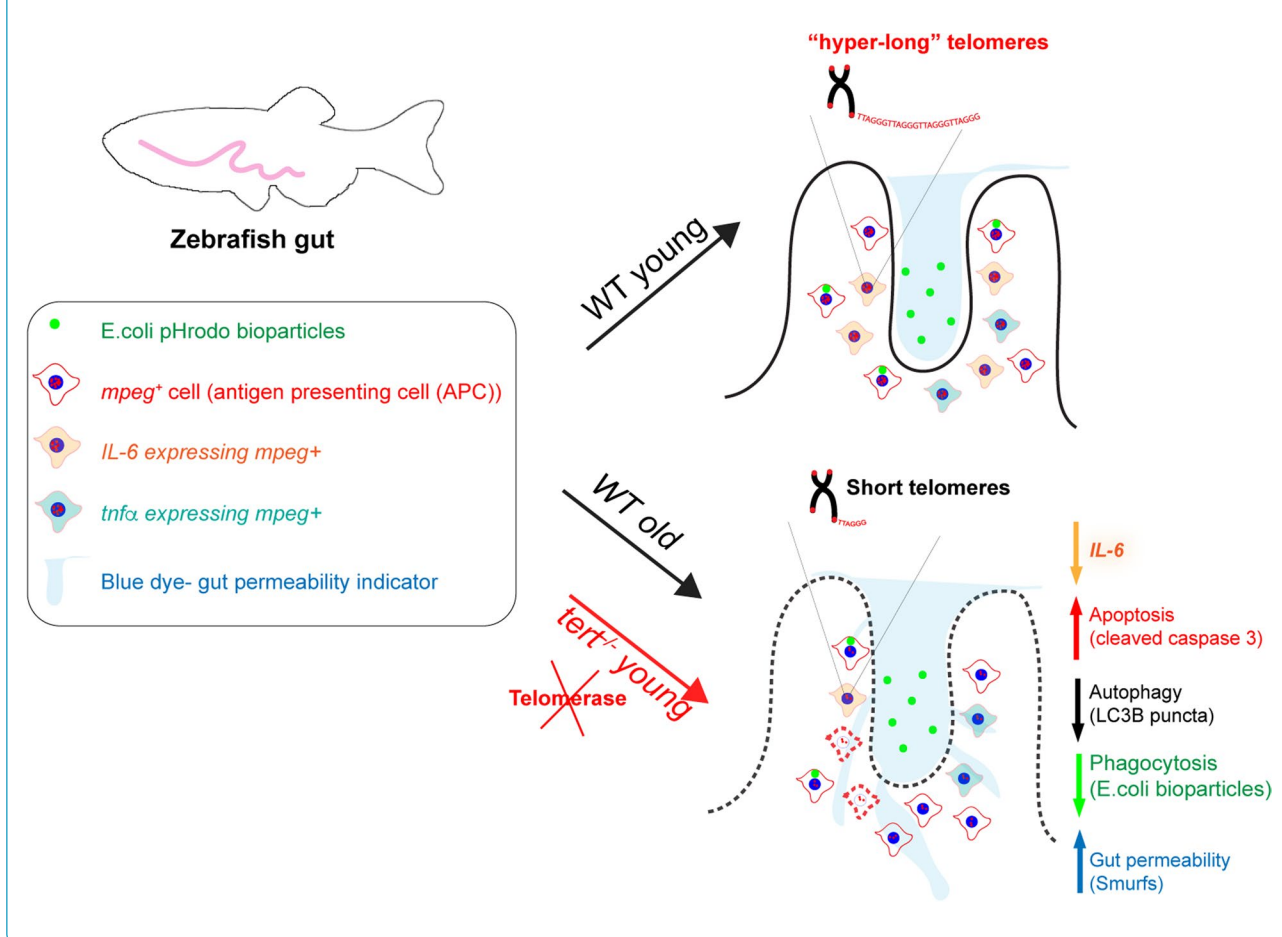
Full list of author information is available at the end of the article



Conclusions: Our data show that limiting levels of telomerase lead to alterations in gut immunity, impacting on the ability to clear pathogens in vivo. These are accompanied by increased gut permeability, which, together, are likely contributors to local and systemic tissue degeneration and increased susceptibility to infection with ageing.

Keywords: Zebrafish, Telomerase, Telomeres, Gut, Immunity, Macrophages, Phagocytosis, Gut permeability

Graphical Abstract



Summary

Our data show that limiting levels of telomerase contribute to alterations in gut immunity, namely increased apoptosis, decreased autophagy and immune activation of *mpeg*⁺ macrophages in the gut. This is accompanied by a decreased ability to clear pathogens and increased gut permeability. Together, these are likely contributors to local and systemic tissue degeneration and susceptibility to infection with ageing.

Introduction

Telomeres are repetitive DNA sequence of TTAGGG that, together with the protein shelterin complex, provide a protective cap at the end of our chromosomes [1].

Telomerase, the reverse transcriptase capable of elongating telomeres, is mostly restricted in somatic cells. However, in humans, due to limited telomerase expression and the “end-replication problem” [2], telomeres shorten with ageing and with each cell-division, leading to proliferative exhaustion and replicative senescence [3–7]. This is thought to contribute to the accumulation of cellular senescence with ageing in humans [8] and senescence has been linked to several age-associated diseases [9]. Telomerase expression is required for the maintenance of germ cells and during embryonic development, thereby ensuring the replicative potential over generations [10]. Telomerase expression is also a hallmark of tissue stem cells, but its expression in these cells is still insufficient to completely prevent telomere shortening over time [11].

Immune cells are somatic cells that break the rule, as they are capable of modulating telomerase expression in a homeostatic manner. It has long been known that telomerase is up-regulated in adaptive immune cells, namely in T and B-cells [12]. Telomerase expression in this setting ensures that T-cells undergoing clonal expansion reduce the rate of telomere attrition; thereby ensuring that the replicative potential required for these proliferation outbursts during the adaptive immune response is maintained throughout most of our lives [13–15]. B-cells have also been described to up-regulate telomerase expression during maturation, a process that also relies on proliferation bursts [16].

Whereas it seems intuitive that a cell-type that depends on regular proliferation outbursts for function may have evolved to modulate telomerase expression, such as stem cells, T cells, B cells and most human cancers [17], it is less obvious why other somatic cells may also do so. Nevertheless this is exactly what a growing body of evidence suggest for a variety of innate immune cells, including neutrophils and macrophages, at least in the context of disease [18–20]. Whether and how telomerase may play a role in innate immune subtypes in the context of natural ageing, in different tissues, however, remains to be determined. Relevantly, telomerase is not only capable of restoring telomeres (canonical function) but also of performing non-canonical functions involved in the regulation of gene expression (recently reviewed here [21]). These so called non-canonical functions of telomerase are important because they are thought to modulate the transcription of genes [22, 23] involved in a wide variety of cellular functions, from DNA repair [24], to enhanced proliferation [25, 26], inhibition of apoptosis [25] enhanced migration [18, 24, 27–31] and inflammation [32–34]. In the nucleus, these non-canonical functions include transcriptional regulation of genes involved in inflammation, including nuclear factor kappa B (NFkB) and tumour necrosis factor alpha (TNF α) [32–34], as well as genes involved in cell proliferation [26, 35] and cell survival [36, 37]. Telomerase can also translocate to the mitochondria, where it has been shown to play a protective role against DNA damage and oxidative stress [38, 39].

The gut is a key tissue where inflammation must be carefully controlled and modulated to prevent disease [40]. It is the largest immune organ in the body [41] and is constantly being exposed to foreign antigens, having therefore to maintain a tolerogenic immune status [42]. Perturbations in gut immune regulation are known to contribute to diseases such as inflammatory bowel diseases (IBD) [43], ulcerative colitis (UC) and Crohn's disease (CD) [44] and indeed

ageing-associated degeneration and dysfunction [45–47], including in zebrafish [48]. Ageing of the gut is an often forgotten ailment in old age that can contribute to malnutrition [49], ageing-associated anorexia and, consequently, sarcopaenia, frailty, loss of independence and resilience [47, 50]. The specific cellular and molecular mechanisms driving changes in inflammation in the gut with ageing, and their relative contribution to the clinical manifestations of an aged gastrointestinal tract, however, are still poorly understood [47]. Previous work in different model organisms, including in zebrafish, has highlighted the gut as one of the first tissues to age in a telomerase-dependent manner. Indeed, there is evidence suggesting that the gut plays an important role in the pathogenesis and progression of systemic inflammation, which can lead to multiple organ failure and eventually death [51–54]. We therefore set out to determine the molecular and functional consequences that whole organism telomerase depletion may have in gut-associated immune cells, in specific. We used the telomerase mutant (*tert*^{-/-}) zebrafish as a model [55–57], alongside its WT counterpart. Zebrafish have been previously shown to age in a telomerase-dependent manner, mimicking many aspects of human ageing [55, 56, 58]. Accordingly, while *tert*^{-/-} fish have a lifespan of c. 12–20 months, WT fish typically die between c. 36–42 months of age [55]. Akin to humans, previous work in zebrafish suggested that telomerase expression is likely to be differentially regulated in different cell types, highlighted by the observation that peripheral and kidney marrow blood cells have much longer telomeres than most other somatic cell types [55, 56].

Here we show that gut immune cells have telomerase-dependent "hyper-long" telomeres, which we identified as being predominantly macrophages/dendritics (*mpeg1.1*⁺, therein called *mpeg*⁺ for simplicity, and *cd45*⁺*mhcII*⁺). We show that a subset of gut *mpeg*⁺ cells express telomerase (*tert*) in young WT zebrafish, but that the relative proportion of telomerase-expressing *mpeg*⁺ cells decrease with ageing. This is accompanied by telomere shortening and a telomerase-dependent decrease in expression of autophagy (LC3B) and immune activation (IL-6) markers in gut *mpeg*⁺ cells with ageing. Importantly, we show that these telomerase-dependent molecular alterations are accompanied by impaired phagocytosis of *E. coli* and increased gut permeability in vivo. Together, our data show that limiting levels of telomerase lead to changes in gut immunity and gut permeability likely to contribute to local and systemic tissue degeneration and susceptibility to infection with ageing [54, 59].

Results

Gut-associated leukocytes have telomerase-dependent “hyper-long” telomeres, independently of proliferation

Previous work using telomere in situ hybridisation (Telo-FISH) in zebrafish gut sections show very distinct cell populations with different telomere lengths, and highlighted a particular subset of cells with “hyper-long” telomeres in the gut, which was not observed in the absence of telomerase (*tert*^{-/-})⁵⁶. Together, these observations suggested that, akin to humans, telomerase expression is likely to be differentially regulated in different cell types in WT zebrafish, but the identity of those “hyper-long” telomere cells in the gut remained to be determined. Importantly, in terms of telomere length in the gut, the most significant difference between WT and *tert*^{-/-} zebrafish at a young age (under 5 months) is the absence of these telomerase-dependent “hyper-long” telomere cells [55, 56]. We therefore postulated that these likely constitute a cellular subset particularly dependent on telomerase, and a potential candidate for driving the initial stages of the ageing phenotypes in the *tert*^{-/-} mutant and, at later stages, in naturally aged WT. Because it had also been shown that peripheral blood and the head kidney (the bone marrow equivalent in zebrafish) had longer telomeres than other tissues in WT zebrafish [55, 56], we hypothesised that these “hyper-long” telomere cells in the gut were likely to be tissue-associated immune cells. We therefore set out to determine what these cells were, and whether they were still present in the *tert*^{-/-} gut, albeit with shorter telomeres.

Our results confirmed the presence of these “hyper-long” telomere cells in WT young adult zebrafish gut and that this strong telomere signal (Telo-FISH) was not detected in the absence of telomerase (*tert*^{-/-}), i.e., that the presence of the “hyper-long” telomeres is telomerase-dependent (Fig. 1A1). Importantly, we show a clear overlap between these “hyper-long” telomere cells and a pan-immune cell marker (L-plastin) in the gut. Importantly, these gut immune cells are still present in

comparable numbers in the absence of telomerase, albeit with much shorter telomeres (Fig. 1A1.1). To discard the possibility that gut immune cells have increased telomeric signal due to cell proliferation and DNA replication in S-phase, we performed a control centromere FISH in parallel to the Telo-FISH. For this, we used a fluorescent PNA probe which we designed to be complementary to a near-centromere region (ZEFRFAL1), shown to be detected consistently and only once per chromosome in the zebrafish genome [60]. If the “hyper-long” telomere cells were replicating, then the “centromeric” signal would also be significantly stronger in these cells. We show that this is not the case (Fig. 1B). Normalising the telomere signal by the centromeric signal (tel/cent ratio) controls for any differences in DNA content. We further normalised our comparisons by dividing the tel/cent ratio of the L-plastin⁺ cells by the tel/cent ratio of the gut epithelial cells (enterocytes) from the same field of view (FOV). This allowed us to be confident when comparing and pooling the results of multiple FOV from multiple animals together. We detected a clear “hyper-long telomere cell population, which we identified having telomere signal between 20 and 50% stronger than epithelial cells in the gut (1.20 to 1.50 tel/cent ratio in L-plastin⁺ normalised to tel/cent ratio of epithelial cells) (Fig. 1B1). Again, we show that, in the telomerase mutant, all cells have a tel/cent ratio below 1.20. Moreover, as has been shown before [56], the cell population within the lower telomere intensity, which we identified as epithelial cells based on the well-described nuclear morphology and localisation in the gut villi, has equivalent telomere signal between WT and *tert*^{-/-} zebrafish. This again strongly suggests that, as in humans, WT zebrafish have restricted telomerase expression/activity in somatic cells. We further confirm that this increased telomere intensity is independent of proliferation by showing that, whereas about 80% of L-plastin⁺ cells have “hyper long” telomeres in a young WT gut (Fig. 1E), under 10% of these cells are proliferating, as assessed by double L-plastin/PCNA

(See figure on next page.)

Fig. 1 Gut-associated leukocytes have telomerase-dependent “hyper-long” telomeres, independently of proliferation: **A** Zebrafish gut paraffin sections **A1** showing telomere TelC-Cy3 CCCTAA PNA probe in situ hybridisation (Telo-FISH) in red, combined with anti L-plastin immunofluorescence, in green. Nuclei counterstaining with DAPI in blue. Representative images shown from young (c.5 months) WT and *tert*^{-/-}. Yellow arrows are pointing to an example of an L-plastin⁺ cell (green cell) **A1.1** Quantifications of the average % of L-plastin⁺ cells per gut villi, average per animal. **B** Representative images of Young WT gut with Telo-FISH combined with a near centromeric probe (ZEFRFAL1), which we call Cent-FISH. **B1** Relative telomere length (Telo-FISH/Cent-FISH signals) quantifications defining the hyper-long telomere population as above 1.20 when normalised to the relative telomere length of nearby villi epithelial cells. **C** Representative images of Young WT gut showing a double immunofluorescence staining against PCNA (white) and L-plastin (red) and **C1** quantifications of the % (from within the L-plastin⁺ cell population) of PCNA⁺L-plastin⁺. Yellow arrows here point to an example of a double positive (PCNA⁺L-plastin⁺) cell. **D** Zebrafish Head kidney paraffin sections, showing telomere TelC-Cy3 CCCTAA PNA probe in situ hybridisation (Telo-FISH) in red, combined with anti L-plastin immunofluorescence, in green. Nuclei counterstaining with DAPI in blue. Representative images shown from young (c.5 months) **D1** WT and **D2** *tert*^{-/-}. Yellow arrows are pointing to an example of an L-plastin⁺ cell (green cell) **E** Quantifications of the % of L-plastin⁺ with hyper-long telomeres comparing young WT gut with corresponding head kidney. **F** Relative telomere length quantification in L-plastin and epithelial cells in gut and Head kidney. All scale bars: 50 μm unless stated otherwise in the figure

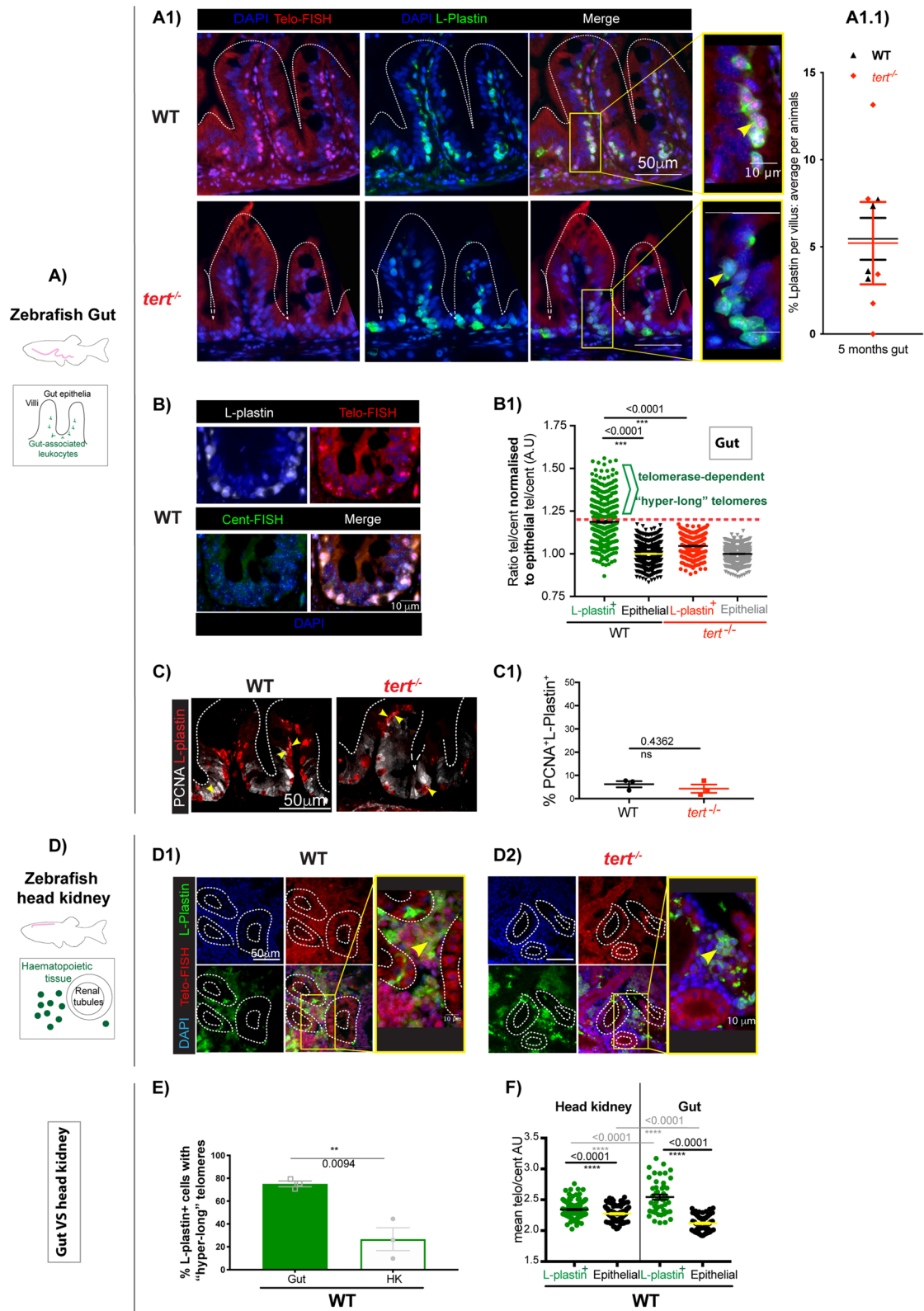


Fig. 1 (See legend on previous page.)

(Proliferating Cell Nuclear Antigen) staining (Fig. 1C). Moreover, contrary to the differences between telomere intensities, there is no significant difference in proliferation between WT and *tert*^{-/-} immune cells (Fig. 1C1).

Even though the zebrafish gut share many similarities with the mammalian gut, including most of its diversity of immune sub-types [61, 62], there are still some key differences [62, 63]. A relevant difference to have in mind for this study is that zebrafish do not have organised lymphoid structures, such as mesenteric lymph nodes (MLN), isolated lymphoid follicles (ILFs) or Peyer's patches (PP). Moreover, the origin of resident gut macrophages, as well as the relative contribution of monocytes from the periphery towards the resident gut population is still largely unknown [61]. Whether there is a constant replenishment from the periphery or whether there is a localised immune stem cell pool or both, and how this may change with ageing, remains to be determined in zebrafish. Therefore, we hypothesised that perhaps these “hyper-long” telomere immune cells had inherited these long telomeres because they had originated in the head kidney marrow. The head kidney marrow can be considered the equivalent of the human bone marrow, and it is the main source of peripheral immune cells in the adult zebrafish [64]. Importantly, it was previously shown that the zebrafish head kidney has predominantly long telomeres, whereas other tissues in zebrafish show a mixture of long and short telomeres [55, 56], supporting the hypothesis.

Our data show that immune cells (L-plastin⁺) also have significantly longer telomeres than epithelial cells in the head kidney (Fig. 1D, E, F). However, immune cells have significantly longer telomeres in the gut than in the head kidney, suggesting that, even if there is a contribution of immune cells from the periphery, there is further telomerase modulation in the gut (Fig. 1E, F).

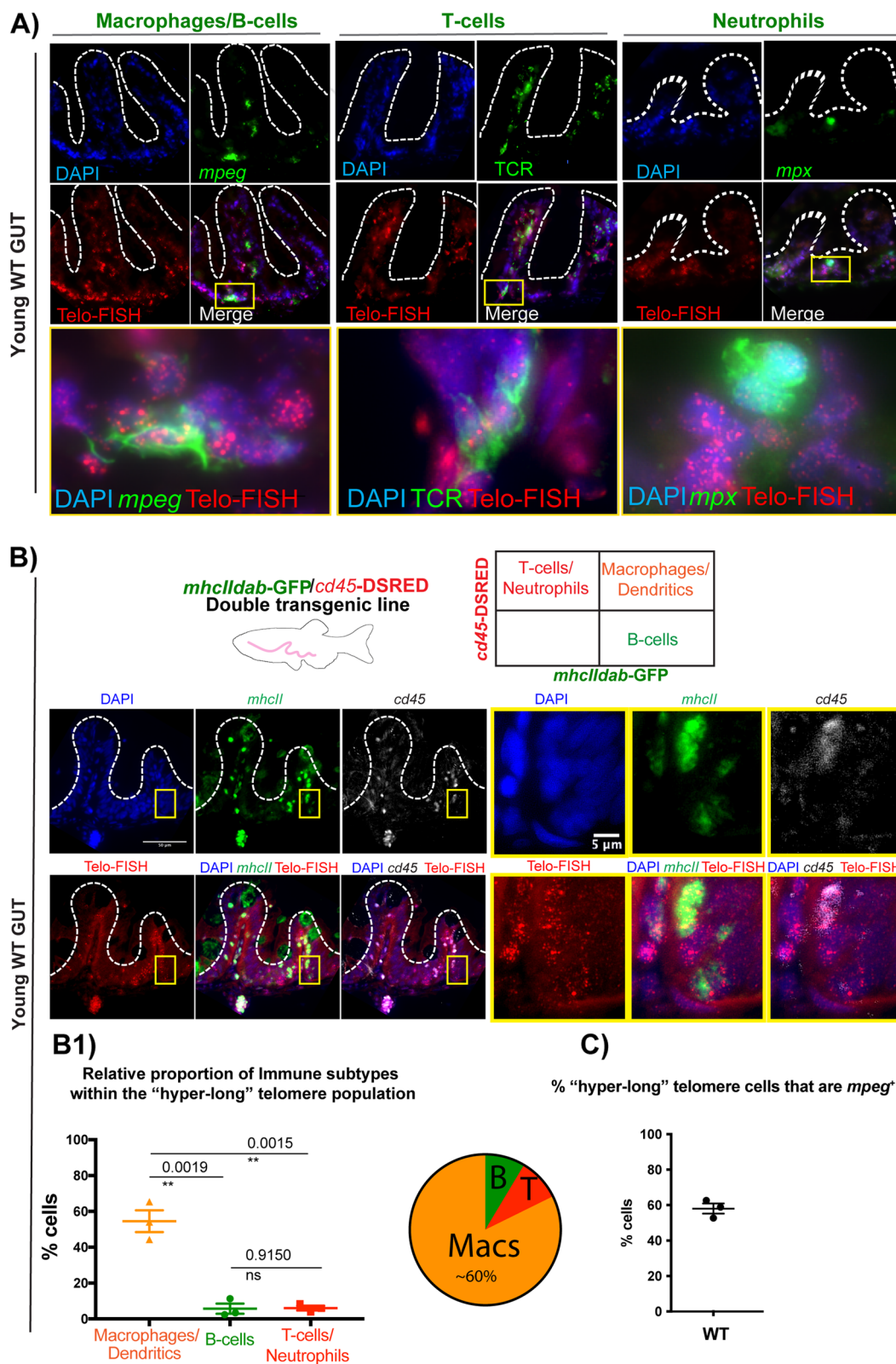
Most “hyper-long” telomere gut-associated leukocytes in zebrafish are macrophages

Since, akin to humans, the zebrafish gut contains cells from both innate and adaptive immune lineages [41, 61, 62, 65–67], we set out to identify the different

subsets of immune cells from within the “hyper-long” telomere gut immune population (L-plastin⁺). To do this, we used a combination of available immune-specific reporter fluorescent transgenic zebrafish lines and immune-specific antibodies alongside Telo-FISH, in WT young adult tissue sections. In specific, we used what has been described as a macrophage-specific reporter (*mpeg1.1:mcherry caax*) [68] and a neutrophil-specific reporter (*mpx:gfp*) [69] transgenics. In addition, we used a zebrafish specific anti-T-cell receptor (TCR) antibody to identify T-cells (Fig. 2A). These three lines allowed us to observe that while putative macrophages (*mpeg*⁺) and T-cells (TCR⁺) both have “hyper-long” telomeres, this is not the case for neutrophils (*mpx*⁺). To further validate the identity of these cells and be able to quantify the relative proportion of these immune subsets from amongst the “hyper-telomere” immune cell population, we used the double transgenic *mhcII:gfp/cd45:dsred* zebrafish line [70]. This line has been reported to allow the identification of macrophages/dendritic cells (*mhcII:dab:gfp⁺cd45:dsred⁺*); B-cells (*mhcII:dab:gfp⁺cd45:dsred⁻*) and T-cells/neutrophils (*mhcII:dab:gfp⁻cd45:dsred⁺*) in the zebrafish gut [70] (Fig. 2B). Using this transgenic line, we calculated that the relative proportion of these immune subsets from within the “hyper-long” telomere length population is constituted by c.60% putative intestinal mononuclear phagocytes (MPs): ((Macrophages (MΦs)/dendritics (DCs) (*mhcII:dab:gfp⁺cd45:dsred⁺*)), c.10% B-cells (*mhcII:dab:gfp⁺cd45:dsred⁻*) and c.10% T-cells (*mhcII:dab:gfp⁻cd45:dsred⁺*) (Fig. 2A and B). Because some recent reports have highlighted that the *mpeg1.1* promoter in transgenic zebrafish may also mark some non-macrophage cells, such as a sub-population of B-cells in the gut [71], we compared the result obtained from the *mhcII:gfp/cd45:dsred* transgenic line with the *mpeg1.1:mcherry caax* line and obtained similar results. In specific, using the *mpeg1.1:mcherry caax* line, we calculated that about 60% of “hyper-long” telomere cells were *mpeg*⁺ in the zebrafish gut (Fig. 2C). Together, these two transgenic lines gave us the confidence to conclude that the majority the “hyper-long”

(See figure on next page.)

Fig. 2 Most “hyper-long” telomere gut-associated leukocytes in zebrafish are macrophages. **A** Telo-FISH (red) combined with anti-RFP antibody to detect *mpeg1.1:mcherry caax*⁺ cells (green), which have been described as mostly macrophages and a subset of B-cells; anti-TCR (green) to detect T-cells and anti-GFP to detect *mpx*:GFP⁺ expressing cells, which have been identified as neutrophils. Boxed areas show in yellow are expanded and displayed in the bottom panels. **B** *mhcII:dab-GFP/cd45-DSRED* transgenic line was used to perform Telo-FISH (red) combined with anti-GFP to detect *mhcII:dab-GFP* and anti-RFP to detect *cd45-DSRED*. Double *mhcII:dab-GFP⁺/cd45-DSRED⁺* have been identified as macrophages or dendritic cells; single *mhcII:dab-GFP⁺* as B-cells and single *cd45-DSRED* as T-cells or neutrophils. Boxed areas show in yellow are expanded and displayed in the right panels. **B1** Quantification of the relative proportion of immune sub-types within the “hyper-long” telomere population, using the transgenic from B). **C** Quantification of the % of “hyper-long” telomere cells that are *mpeg*⁺, using the *mpeg1.1:mcherry caax* transgenic from A. All animals are WT for telomerase, and are of a young age (c.5 months). Nuclei are counterstained with DAPI (blue) and all scale bars represent 50 μm, unless stated otherwise in the figure



telomere cells in the zebrafish gut are likely to be intestinal mononuclear phagocytes (MPs) or macrophages.

A subset of WT gut *mpeg*⁺ cells express telomerase (*tert*) but the relative proportion of these cells decreases with ageing and is accompanied by telomere shortening

If indeed, as our data so far suggest, there is a further modulation of telomerase in gut immune cells, and that the majority of the “hyper-long” telomere cells in the gut are macrophages, then we would expect to detect telomerase expression in these cells. Additionally, since these “hyper-long” telomeres are telomerase-dependent, and telomeres have been shown to shorten with ageing in zebrafish [55], then you would hypothesise that whatever telomerase expression may exist in these cells in a young WT gut, it is likely to decrease in ageing. To test these hypotheses, we used the *mpeg1.1: mcherry caax* line and combined anti-RFP (to detect mcherry) immunofluorescence with telomerase (*tert*) mRNA fluorescent in situ hybridisation in young adult (c.5 months) and old WT (>36 months) zebrafish tissue sections. We also combined this with anti-PCNA immunofluorescence staining to be able to distinguish between proliferating and non-proliferating cells (Fig. 3A).

Our data show that about 30% of *mpeg*⁺ cells express *tert* in WT young, compared to about 10% in WT old zebrafish gut (Fig. 3A1), supporting the hypothesis that at least a subset of these cells expresses telomerase (*tert*) at a given point, and that the number of telomerase-expressing cells decreases with ageing. Accordingly, we observe a decrease in relative telomere length (telo/cent ratio) in gut *mpeg*⁺ cells with ageing (Fig. 3C), C1) and a decrease in the proportion of *mpeg*⁺ cells with “hyper-long” telomeres (Fig. 3C2). We also observe these decreases when analysing the bulk of gut immune cells (L-plastin⁺), rather than just *mpeg*⁺ cells (Supp Fig. 1), suggesting that there is a general decrease in telomerase expression in gut immune cells with ageing (or a decrease in the proportion of immune cells that can up-regulate telomerase, with ageing). Relevantly, in young WT zebrafish gut,

only about 10% of telomerase-expressing macrophages were proliferating (*mpeg*⁺ *tert*⁺ PCNA⁺) and we did not detect any significant difference in the proportion of these cells between young and old. Together, these data show that even though a proportion of gut *mpeg*⁺ cells express telomerase at young ages, the proportion of telomerase-expressing cells decreases with ageing and is accompanied by telomere shortening. Decreased telomerase expression and telomere shortening in these cells does not impact the level of proliferation of *mpeg*⁺ cells, or immune cells in general (Supp Fig. 2), suggesting that the expression of telomerase in these cells may have evolved to serve other non-canonical functions, rather than maintenance of replicative potential.

Telomerase depletion accelerates age-associated increased apoptosis, decreased autophagy and decreased immune activation of zebrafish *mpeg*⁺ gut cells

Telomerase has been described to have both canonical (telomere elongation) and non-canonical (telomere elongation-independent) functions. We therefore set out to determine the key molecular changes occurring in gut *mpeg*⁺ cells in the absence of telomerase (*tert*), at the young age of c.5 months, where the levels of critically short telomeres are not yet sufficient to induce a significant accumulation of DNA damage response markers [56, 72]. This means that most changes that we detect in the gut of young *tert*^{-/-} animals are more likely to be due to absence of *tert* itself and its non-canonical functions, rather than telomere-induced DNA damage. We therefore chose to monitor potential non-canonical changes, such as autophagy and immune activation markers, as well as classic molecular targets that would be expected to change in response to short telomeres, such as proliferation and DNA damage. Importantly, we asked whether these alterations were also occurring with natural ageing and, if so, whether telomerase depletion accelerated such phenotypes, as this would indicate that such ageing phenotype are telomerase-dependent. Our results show that there is

(See figure on next page.)

Fig. 3 WT zebrafish gut *mpeg*⁺ cells express telomerase but this decreases with ageing and is accompanied by telomere shortening. The *mpeg1.1: mcherry caax* transgenic zebrafish line was used to **A** detect telomerase (*tert*), by RNA in situ hybridisation (white) and PCNA expression in gut *mpeg*⁺ cells in young and old WT zebrafish paraffin sections. **A1** Quantification the % of *mpeg*⁺ with *tert* expression and no PCNA expression (green) and the % of *mpeg*⁺ cells with PCNA expression (magenta). Yellow arrows are pointing to a *mpeg*⁺ cell example (in green), that is expressing *tert* (white dots) and that is either PCNA negative (top) or PCNA positive (bottom) In **B** The relative % of *mpeg*⁺ cells with telomerase are compared between the gut and the head kidney of young WT fish. **C** The *mpeg1.1: mcherry caax* transgenic zebrafish line was used to detect telomeres using Telo-FISH (red), Cent-FISH (white) combined with anti-RFP (in green) to detect *mpeg*⁺ cells young and old WT zebrafish paraffin sections. Yellow arrows here are pointing to *mpeg*⁺ cells (green) identified in the panel showing *mpeg* and arrows were kept when the other channels are displayed for ease of identification of where the *mpeg*⁺ cells would be. Merged channels can be seen in the last panel on the right. **C1** Shows the relative quantification of telomere length (tel/cent ratio) in gut *mpeg*⁺ cells in WT young and old, compared to young *tert*^{-/-} zebrafish. **C2** Shows the % of gut *mpeg*⁺ cells with “hyper-long” telomeres. Young animals are c.5 months old and old animals are >30–36 months old. Nuclei are counterstained with DAPI (blue). All scale bars represent 50 μm unless otherwise stated in the figure

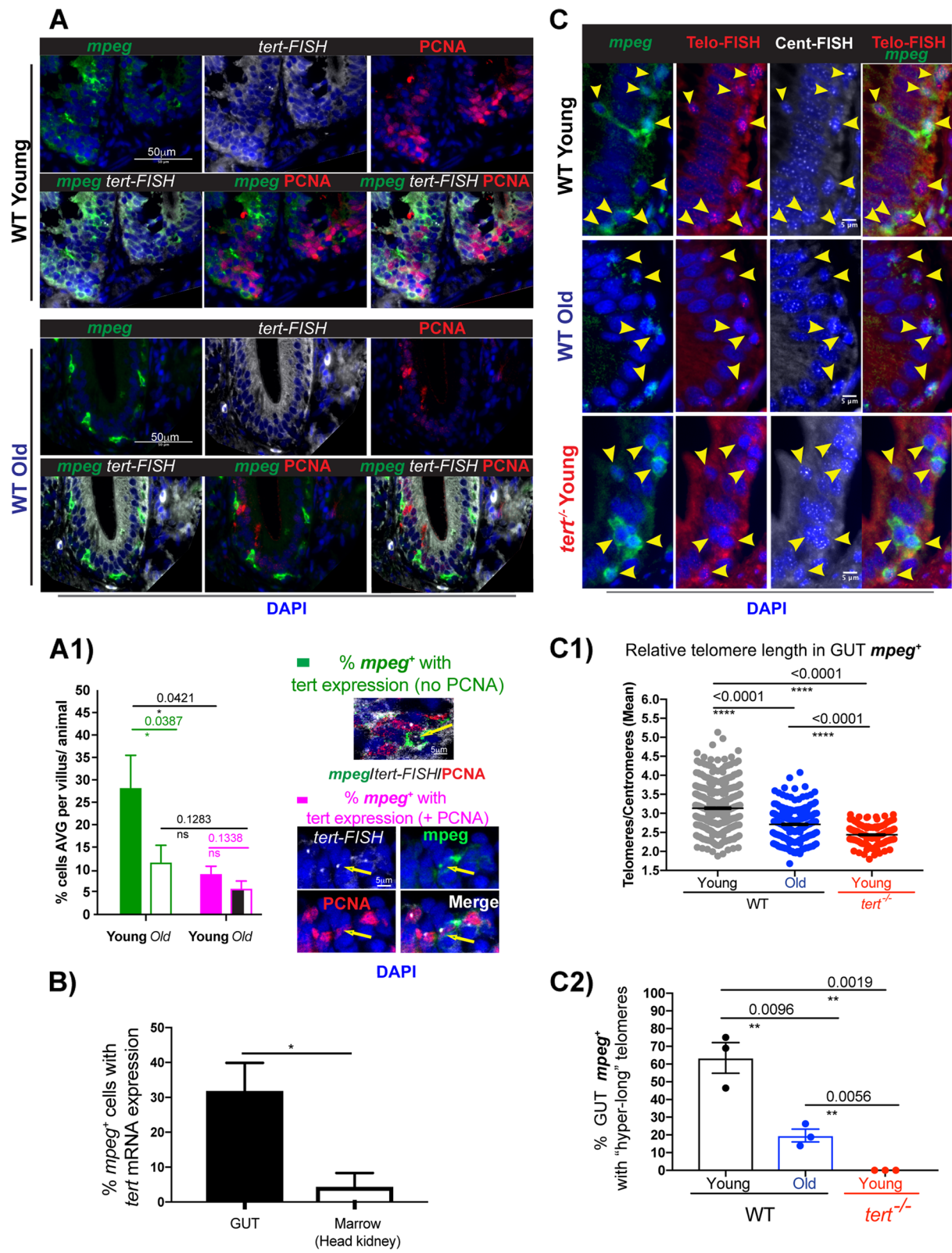


Fig. 3 (See legend on previous page.)

a significant decrease in the numbers of *mpeg*⁺ cells in the gut in old age, but that this is not significantly accelerated in the absence of telomerase, at least at the young age that our work is focusing on. (Fig. 4A), A1)). In accordance with our previous observation that telomerase expression does not significantly affect gut immune cell proliferation (Fig. 1C), C1)), we also do not detect significant changes in gut *mpeg*⁺ proliferation in either *tert*^{-/-} or natural ageing (Fig. 4A), A2)). Even though we observe an increase in DNA damage response markers, namely gH2AX, with ageing, this is not accelerated in the absence of telomerase, in the young *tert*^{-/-}, as has been reported before [55, 56] (Fig. 4B), B1)). We do, however, observe a significant increase in cleaved caspase 3⁺/*mpeg*⁺ cells with ageing, and this observation is accelerated in the absence of telomerase (*tert*^{-/-}), suggesting, that depletion of telomerase is contributing to this, i.e., that it is a telomerase-dependent mechanism (Fig. 4C), C1)).

Because autophagy is a key molecular mechanism for immune function and telomerase has been shown activate autophagy in different cells types [73–76], we hypothesised that gut macrophage autophagy would be affected in the absence of telomerase. Our data show that there is a significant decrease in autophagosomes, as assessed by LC3B puncta, in the *mpeg*⁺ gut cell population with old age, which again is accelerated in the absence of telomerase (Fig. 4D), D1)). This suggests that telomerase contributes to the regulation of autophagy in gut *mpeg*⁺ cells and telomerase depletion is likely to contribute to autophagy defects in these cells in old age. Finally, we tested for the expression of key immune activation markers, known to be important for gut macrophage function, namely TNFα and IL-6. For this, we used the *mpeg*⁺: *mcherry* line crossed with the *TgBAC* (*tnfa*:GFP) [48] and an anti-IL-6 antibody. Our data show that old age is associated with decreased numbers

of *tnfa* expressing *mpeg*⁺ cells, as well as a decreased numbers of IL-6 expressing *mpeg*⁺ cells (Fig. 4E), E1), F), F1)). In specific, we further show that decreased numbers of IL-6 expressing *mpeg*⁺ cells is accelerated in the absence of telomerase (*tert*^{-/-}), suggesting that this is a telomerase-dependent mechanism.

Telomerase depletion leads to impaired phagocytosis in *mpeg*⁺ cells in vivo and increased gut permeability

As the name indicates, a key role, even if not the only one, for intestinal mononuclear phagocytes (MPs) is to phagocytose [40]. A remarkable characteristic of gut MPs is their ability to phagocytose foreign material without generating an inflammatory response, and gut macrophages do not fall within the M1/M2 classic phenotypes. This ability is essential in their role in discriminating between pathogens and other non-harmful antigens, such as food and microbiota [40]. It was therefore difficult to predict whether the changes observed in the numbers of *mpeg*⁺*tnfa*⁺ and *mpeg*⁺IL-6⁺ with ageing, and, in the case of IL-6, accelerated in the *tert*^{-/-}, would lead to changes *mpeg*⁺ function. Nevertheless, both IL-6 and TNFα have been described to play a role in macrophage's immunosurveillance ability [77, 78]. To test whether immunosurveillance was affected in the zebrafish gut with old age, and whether this was telomerase-dependent, we adapted the well-described *E.coli* phagocytosis assay, using pHrodo™ Green *E. coli* BioParticles™ Conjugate for Phagocytosis [70]. We adapted this assay to assess phagocytosis specifically in the gut, in vivo. For this, we optimised delivery of these particles via oral gavage in adult *mpeg*⁺: *mcherry caax* zebrafish, both at young (c.5 months) and old (c. 35 months) WT ages, and in the absence of telomerase (*tert*^{-/-}) at c.5 months. *mpeg*⁺ cells can be detected by the membrane-bound *mcherry caax* and the % of *mpeg*⁺ cells containing visible green *E.coli* bioparticles inside

(See figure on next page.)

Fig. 4 Telomerase depletion accelerates age-associated increased apoptosis, decreased autophagy and decreased immune activation of zebrafish gut *mpeg*⁺ cells. The *mpeg1.1*: *mcherry caax* transgenic zebrafish line was used to assess **A** numbers (**A1**) and percentage of proliferation (**A2**) of gut *mpeg*⁺ cells, using double immunofluorescence staining against RFP to detect *mpeg1.1*: *mcherry caax* (red) and anti-PCNA (white) to detect proliferating cells. Yellow arrows in A) are pointing to examples of *mpeg*⁺ cells (red) that are also PCNA⁺ (white). Using the same fish (*mpeg1.1*: *mcherry caax*), we further analysed: **B** DNA damage response (DDR), using double immunofluorescence against RFP to detect *mpeg1.1*: *mcherry caax* (red) and gH2AX (white) to detect DDR. Yellow arrows in B) are pointing to examples of *mpeg*⁺ cells (red) that are also gH2AX⁺ (white). **B1** Quantification of the % of *mpeg*⁺ gH2AX⁺ cells; **C** Apoptosis, using double immunofluorescence against RFP to detect *mpeg1.1*: *mcherry caax* (red) and anti-cleaved caspase 3 (white) to detect apoptotic cells. Yellow arrows in C) are pointing to examples of *mpeg*⁺ cells (red) that are also cleaved-caspase 3⁺ (white). **C1** Quantification of the % of *mpeg*⁺ cleaved-caspase 3⁺ cells; **D** Autophagy, using double immunofluorescence against RFP to detect *mpeg1.1*: *mcherry caax* (red) and LC3B (white) to detect autophagosomes. Yellow arrows in D) are pointing to examples of *mpeg*⁺ cells (red) that are also LC3B puncta⁺ (white). **D1** Quantification of the % of *mpeg*⁺ LC3B⁺ cells. *tnfa*: eGFP-F/*mpeg1.1*: *mcherry caax* fish were used to assess immune activation, **E** using double immunofluorescence against RFP to detect *mpeg1.1*: *mcherry* (red) and anti-GFP (white) to detect *tnfa* expressing cells. Yellow arrows in E) are pointing to examples of *mpeg*⁺ cells (red) that are also *tnfa*⁺ (white). **E1** Quantification of the % of *mpeg*⁺ *tnfa*⁺ cells; **F** using double immunofluorescence against RFP to detect *mpeg1.1*: *mcherry caax* (red) and anti-IL-6 (white) to detect IL-6 expressing cells. Yellow arrows in F) are pointing to examples of *mpeg*⁺ cells (red) that are also IL-6⁺ (white). **F1** Quantification of the % of *mpeg*⁺ IL-6⁺ cells. Nuclei are counterstained with DAPI (blue) and all scale bars represent 50 μm unless otherwise stated in the figure

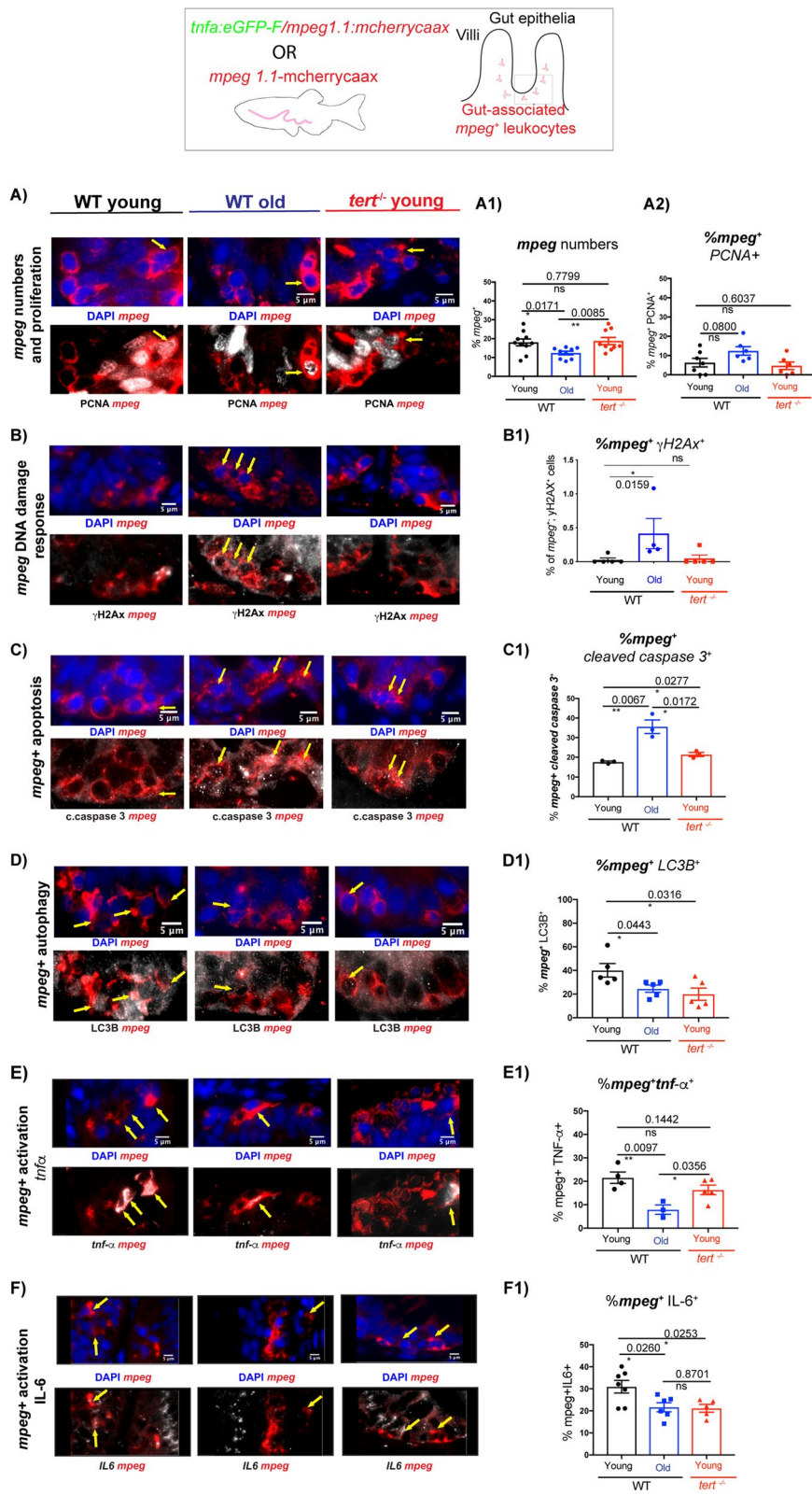
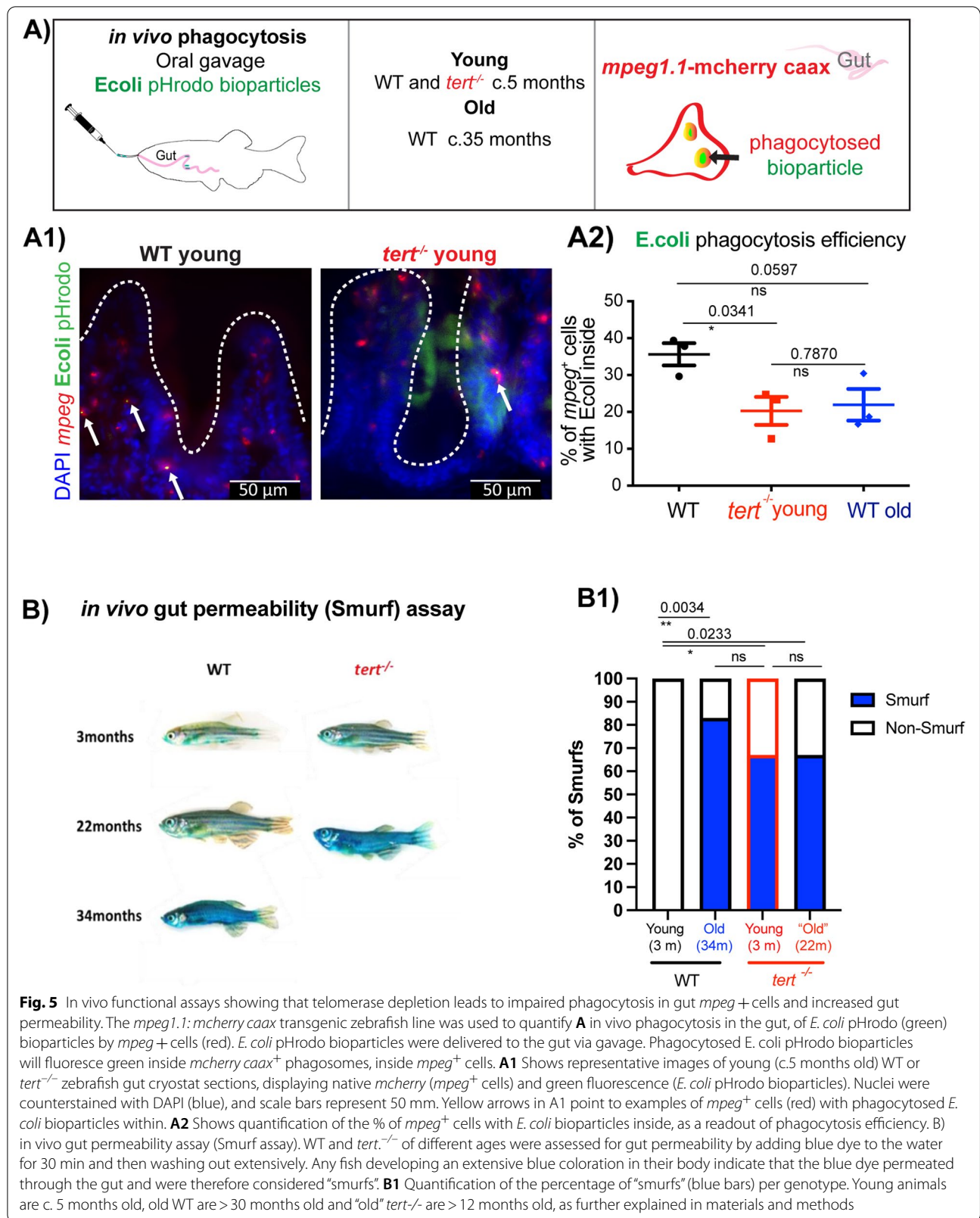


Fig. 4 (See legend on previous page.)



were quantified, as a readout for phagocytosis efficiency (Fig. 5A) A1) (the zebrafish gastrointestinal tract is not acidic [62], so the pHRodo moiety ensures that these particles increase their fluorescence once phagocytosed into acidic vesicles). Our data show that whereas there is a trend towards decreased phagocytosis efficiency in WT old fish ($p=0.0597$) there is a clear statistically significant difference in phagocytosis efficiency in the absence of telomerase ($p=0.0341$) (Fig. 5 A2)). This suggests that telomerase is required for efficient gut *mpeg*⁺ phagocytosis.

Cytokine expression in the gut is key to maintain gut homeostasis and regulate permeability, and most cytokine expression comes from innate immune cells. Because we observed a decrease in gut *mpeg*⁺ cells expressing *tnfa* and IL-6 with ageing, and decreased expression in IL-6, in particular, was accelerated in the absence of telomerase, we set out to test whether telomerase depletion affected gut permeability, a well described phenomena in old age and predictor of mortality in different organisms, including zebrafish [79]. Both IL-6 and TNF α expression by gut macrophages performs more complex functions than just being a pro-inflammatory cytokine. TNF α has been described to be involved in the regulation of enterocyte growth and can affect gut permeability [80]. TNF α can stimulate the production of matrix metalloproteinases and other tissue remodeling enzymes in the intestinal mesenchymal cells, central to regulating epithelial cell function [81]. Alternatively, IL-6 and TNF α expressing macrophages can contribute to the development of pro-inflammatory IL-17 expressing T-helper cells [82]. Previous work, including our own, had shown that gut permeability increases in naturally aged zebrafish. Whether telomerase played a role in this, remained to be determined. We used the well-described Smurf assay [79, 83, 84], and show that indeed, depletion of telomerase accelerated the increase in gut permeability observed in old age (Fig. 5B), B1), as assessed by the proportion of blue fish (Smurfs), in agreement with previous reports [79, 84].

Discussion

The specific cellular and molecular mechanisms driving changes in immunity and inflammation in the gut with ageing, and their relative contribution to the clinical manifestations of an aged gastrointestinal tract are still poorly understood [47]. Telomere dysfunction is a primary hallmark of ageing, and there is evidence suggesting that the gut is one of the first tissues to age in a telomerase-dependent manner, with potential consequences for systemic ageing [54, 55, 85]. However, the consequences of ageing and, in specific, of telomere dysfunction in the immune component of the gut remain largely unexplored.

We set out to determine the molecular and functional consequences of whole organism telomerase depletion to gut-associated immunity, using the zebrafish model [55–57]. Zebrafish has been established as an important complementary model of ageing, since, similarly to humans, requires telomerase for health and lifespan [55, 56, 58, 86]. In this work, we show that gut-associated immune cells have telomerase-dependent “hyper-long” telomeres. In fact, the only significant difference in telomere length between WT and *tert*^{-/-} zebrafish at a young age (c. 5 months) is the absence of these telomerase-dependent “hyper-long” telomere cells (Fig. 1 and in previous work [55, 56]). We therefore postulated that these constituted a cellular subset particularly dependent on telomerase, and were therefore a potential candidate for driving the initial stages of telomerase-dependent ageing phenotypes, i.e. that are accelerated in the absence of telomerase, in the young *tert*^{-/-} model [55]. We therefore focused our study on the young *tert*^{-/-}, and compared it with young and naturally aged WT, to address what molecular and functional changes occurring with age were already accelerated in the absence of *tert* at a young age, before the most severe gut degenerative phenotypes were apparent and any significant telomere-induced DNA damage was detected [55, 56].

Here, we show that gut “hyper-long telomere” immune cells are predominantly macrophages (*mpeg*⁺ or *mhcII*⁺/*cd45*⁺) and that the presence of these long telomeres is telomerase-dependent. Due to limitations in the availability of cell-surface immune-specific antibodies that work in zebrafish, we cannot exclude that we may be missing further smaller specific subsets from within the “hyper-long” telomere population. In accordance with the presence of telomerase-dependent “hyper-long” telomeres, we show that a subset of gut macrophages (*mpeg*⁺) expresses telomerase (*tert*) in young WT zebrafish. Importantly, though, the relative proportion of telomerase-expressing macrophages decreases with ageing and this is accompanied by an overall decrease in relative telomere length. This occurs in *mpeg*⁺ cells, but also in immune cells in general (L-plastin⁺). Together, this data suggest that whatever telomerase is expressed in gut immune cells and, in specific, in *mpeg*⁺ macrophages, is not sufficient to prevent telomere shortening over time. This may be because the expression of telomerase decreases or it may be that there is a progressive inability of activating telomerase with ageing, as has been described to be the case for memory T-cells, which become defective in their ability to proliferate with ageing [14, 87]. However, in the case of gut *mpeg*⁺ cells, or indeed of gut immune cells in general, only a very small proportion of cells is proliferating at a given moment (c.10%). Moreover, this is not significantly affected with

ageing or absence of telomerase. It may be that, even though only a small proportion of the immune cells are proliferating at any given time, this is still enough to contribute to telomere shortening. Moreover, even though we detect only a small % of immune cell proliferation at a given time, or within 3 days of an EdU chase (Supp. Figure 2), we cannot exclude that there may have been more proliferation taking place, for example in immune progenitor cells, whether locally or in the head kidney. In fact, when we compare the telomere shortening in these cells with the telomere shortening in epithelial cells, which are constantly derived from proliferating progenitors, we observe that, even though immune cells' telomeres remain significantly longer than those in epithelial cells, they seem to shorten at a similar or potentially higher rate (Supp Fig. 2). It could also be that other mechanisms are augment telomere shortening, so that they are not linearly shortening in relation to proliferation. For example, it may be that decreased autophagy in gut immune cells, or at least, as our data suggest in *mpeg*⁺ cells, is leading to an accumulation of oxidative stress in these cells, which is a known contributor to rapid telomere attrition [88]. In fact, it has been shown that late generation telomerase null mice display altered mitochondria metabolism and increased oxidative stress in lung macrophages [89]. This could contribute to a much more significant telomere shortening than you would expect from a linear replicative telomere attrition, even in low proliferating cells [88]. Importantly, the two hypotheses of either gut-associated immune cells being constantly replenished from progenitors deriving from the periphery where they have undergone proliferation or them being slowly proliferating in situ but this being sufficient to drive significant telomere shortening due to damage at telomeres, are not mutually exclusive. In fact, mice gut-associated macrophages have been shown to be composed of locally proliferating progenitors and monocytes derived from the periphery, which are regularly replenished [90].

It is also of note that, even though *tert*^{-/-} gut immune cells' (L-plastin⁺) relative telomere length is much shorter, they are still statistically significantly longer than *tert*^{-/-} gut epithelial cells. This could potentially be due to alternative mechanisms of telomere length (ALT) being present, which have been suggested to co-exist alongside telomerase in zebrafish [91, 92]. It could also simply reflect the fact that *tert*^{-/-} derive from a *tert*⁺ in-cross, since *tert*^{-/-} zebrafish are infertile [56, 58], therefore meaning that there is maternal contribution of telomerase expression during development. If these immune cells are seeded in the gut during development, as is the case for other tissue resident immune cells, such as the liver [93], and given that they are lowly proliferating, they

may have maintained relatively longer telomeres which may be sufficient to maintain relatively longer telomeres in low proliferating cells. Future work performing cell lineage tracing experiments will be required to determine the origins and maintenance mechanisms of adult, gut-associated immune cells.

Telomerase expression in innate immune cells has been shown to correlate with poor prognosis in age-associated, inflammation-driven diseases such as atherosclerosis [19] and in unstable coronary plaques [20]. Furthermore, a study showed that transient transfection of macrophages with telomerase was sufficient to up-regulate matrix metalloproteinase (MMP) secretion, contributing to the tissue-damage characteristic of this disease [18]. Together, these data suggest that telomerase can contribute to the chronic activation and survival of macrophages thereby contributing to inflammation-driven diseases. In contrast, however, telomerase expression could also contribute to an anti-inflammatory state, by maintaining long-telomeres. When processed during DNA replication, telomeric sequences can bind to cytoplasmic Toll-Like Receptor 9 (TLR9), blocking downstream activation of pro-inflammatory pathways [94]. Indeed, recent work shows that synthetic telomeric sequences can modulate cellular energetics and can shift mice macrophages into a metabolically quiescent state, via mTOR regulation [95].

Our data show that, in the absence of telomerase, there are a variety of molecular mechanisms that are altered in gut *mpeg*⁺ cells. Some of these mechanisms are what you would expect from depletion of telomerase. In specific, we observe a decrease in telomere length over-time in gut *mpeg*⁺ cells, increased DNA damage response and apoptosis with ageing. However, the increase in DNA damage response is not accelerated in the young *tert*^{-/-}, suggesting that, at least at this age, and despite the shorter telomeres, it is still not sufficient to accumulate significant, unresolved, DNA damage. Moreover, we do not observe significant telomerase-dependent decrease in gut macrophage (*mpeg*⁺) proliferation with ageing, which would be another obvious consequence of telomerase-dependent telomere shortening. Some of the molecular changes we observe, however, are not necessarily the ones you would expect from telomere-shortening dependent, replicative senescence^{5,6,86}. Instead, they may be better explained by non-canonical functions of telomerase. Telomerase is not only capable of restoring telomeres (canonical function) but also of performing non-canonical functions involved in the regulation of cell survival, inflammation and autophagy⁷³⁻⁷⁶ (recently reviewed here²¹). Here, we identified a telomerase-dependent decrease in autophagosomes (LC3B puncta) in gut *mpeg*⁺ cells with ageing. Additionally, we show that there is a decrease in *tnfa* and IL-6 expressing gut

macrophages (*mpeg*⁺) with ageing, and that the decrease in *mpeg*⁺IL-6⁺ cells, in specific, is accelerated in the absence of telomerase. One could then hypothesize that these are likely consequences of restriction of the non-canonical functions of telomerase. Determining the relative contribution of canonical versus non-canonical telomerase functions in gut macrophage function in ageing will, however, require future studies.

In vivo, a key feature of gut immunity is the ability to phagocytose pathogens. Our data show that the phenotypes we observed in the absence of telomerase accompany phagocytic defects in gut *mpeg*⁺ cells in vivo. The fact that phagocytic defects are not as significant in old age suggest that there may be only partial dependency on telomerase for this function in ageing or, as our data suggest, that there are still some *mpeg*⁺ cells expressing telomerase in old age. Indeed, our data show that there is a c.50% reduction in telomerase-expressing *mpeg*⁺ cells, from c.40% to 20%, and this could explain this observation. If and which the telomerase-dependent deregulated mechanisms here described is the actual cause of impaired phagocytosis remains to be determined. Nevertheless, changes in autophagy and immune activation are good candidates for affecting phagocytosis efficiency. As an example, deregulated LC3-dependent autophagy has been reported to affect macrophage phagocytosis and polarisation (recently reviewed here [96]). In specific, autophagy is important in the recycling of cellular components and Adenosine Tri-phosphate (ATP), thereby contributing to the energy requirements of macrophage activation [97]. In fact, inhibiting autophagy with 3-methyladenine (3-MA) led to decreased levels of IL-6 and TNF- α in mice [96]. Furthermore, the fact that autophagy and phagocytosis share the requirement of several genes in macrophages contributes to the hypothesis that a mechanism, such as telomerase, that affects one may also likely affect the other [98]. The molecular mechanisms regulating autophagy and phagocytosis in adult zebrafish gut macrophages, however, remain largely unknown, adding an extra challenge to dissecting the specific pathways responsible for this phenotype in this study.

Finally, we aimed to determine how the age and/or telomerase-dependent changes we identified in gut immunity could impact on tissue degeneration with ageing. Key telomerase-dependent ageing phenotypes previously described in zebrafish include gut villi atrophy and accumulation of senescent cells. Additionally, previous studies also show increased thickness of the lamina propria, alongside augmented periodic acid Schiff (PAS) staining, both indicative of de-regulated inflammation [54, 55, 99]. However, TNFa and IL-6 expression by gut macrophages perform more complex functions than

just being a pro-inflammatory cytokine. For example, TNFa can stimulate the production of matrix metalloproteinases and other tissue remodelling enzymes in the intestinal mesenchymal cells, central to regulating epithelial cell function [81]. TNFa has also been described to be involved in the regulation of enterocyte growth and can affect gut permeability [80]. Gut permeability has been highlighted as a key phenotype of ageing that closely associates with mortality. Accordingly, our data show an increase in gut permeability with ageing, and this was accelerated in the absence of telomerase, from an early age. However, our data show a decrease in gut *mpeg*⁺ cells expressing TNFa, with ageing, but this was not accelerated in the absence of telomerase, at the early ages tested. This suggests that the telomerase-dependent increase in gut permeability observed is likely not due to TNFa alterations in *mpeg*⁺ cells. It could still, however, be caused by a systemic increase in TNFa in circulation, which was not addressed in this study, but has been previously described to increase with ageing, in humans [100, 101] and mice [102]. Intriguingly, it is known that IL-6 can increase gut permeability by modulating tight junction permeability [103]. Our data, however, show a decrease in IL-6 expressing *mpeg*⁺ cells. We were not however capable of quantifying how much IL-6 was being produced by *mpeg*⁺ cells overall, so it is still a possibility that overall levels of IL-6 are increased. Increased IL-6 levels have in fact been reported to increase in the serum of aged mice [102]. A further hypothesis for how the telomerase-dependent changes in gut immunity here described to contribute to increased gut permeability is that decreased immune activation leads to, not only impaired *E. coli* phagocytosis but also impaired clearance of senescent cells. Previous studies have shown that macrophages are capable of clearing senescent cells in some contexts (recently reviewed here [104]) and that, with ageing, macrophages themselves can acquire senescent-like markers, including an M2-like phenotype [105]. Additionally, senescent-like macrophages have also been shown to induce senescence in other cells in a paracrine fashion, known as the “bystander effect”, thereby capable of amplifying the accumulation of senescent cells *in vivo* [106, 107]. The phenotypes we observe here are in fact consistent with an increased senescent macrophage pool, with decreased numbers of M1-like (*tnfa*⁺ and/or IL-6⁺). Accumulation of senescence has been previously described to occur with ageing, in zebrafish, in a telomerase-dependent manner [55]. The senescence associated secretory phenotype has been described to include matrix metalloproteinases (MMPs), which are potential candidates for tissue destruction and could be involved in affecting gut permeability [108]. Additionally, impaired pathogen clearance may also lead to changes in the

microbiome, which has also been implicated in disrupting intestinal permeability [109, 110].

Conclusions

Together, our data show that limiting levels of telomerase contribute to alterations in gut immunity, impacting on gut permeability and the clearance of pathogens *in vivo*. We therefore highlight telomerase (*tert*) as a key regulator of gut immune functions, likely to contribute to the genesis of gut degeneration and, potentially, systemic alterations, with ageing. Future work using cell-specific manipulation of telomerase will be required to test the requirement and sufficiency of telomerase depletion (canonical and non-canonical) in gut immunity to both local and systemic phenotypes of old age.

Materials and methods

Zebrafish husbandry

Zebrafish were maintained at 27–28°C, in a 14:10 h (h) light–dark cycle and fed twice a day. All experiments were performed in Home Office approved facilities at the Bateson Centre, at the University of Sheffield. All animal work was approved by local animal review boards, including the Local Ethical Review Committee at the University of Sheffield (performed according to the protocols of Project Licence 70/8681 and PP445509).

Zebrafish strains, ages and sex

Four strains of adult zebrafish (*Danio rerio*) were used for these studies: wildtype (WT; AB strain), *tert*^{-/-} (*tert*^{AB/hu3430}), *Tg(mpeg1:mCherryCAAX)sh378* and *Tg(mpx:gfp)* (Source: University of Sheffield); *TgBAC(trfa:GFP)pd1028*⁴⁸ (Source: Bagnat lab, Duke University, USA), crossed with the above mpeg Tg line to produce a double transgenic line (Source: University of Sheffield). All of mixed sexes. Wild-type (WT; AB strain) were obtained from the Zebrafish International Resource Center (ZIRC). The telomerase mutant line *tert*^{AB/hu3430} was generated by *N*-ethyl-nitrosourea mutagenesis (Utrecht University, Netherlands; Wienholds, 2004). It has a T→A point mutation in the *tert* gene and is available at the ZFIN repository, ZFIN ID: ZDB-GENO-100412-50, from ZIRC. The fish used in this study are direct descendants of the ones used previously [29, 30], by which point it had been subsequently outcrossed five times with WT AB for clearing of potential background mutations derived from the random ENU mutagenesis from which this line was originated. The *tert*^{hu3430/hu3430} homozygous mutant is referred to in the paper as *tert*^{-/-} and was obtained by in-crossing our *tert*^{AB/hu3430} strain. Genotyping was performed by PCR of the *tert* gene [29, 30]. The telomerase null mutant (*tert*^{-/-}) zebrafish, extensively

characterised elsewhere [29–31, 72], displays no telomerase activity and has significantly shorter telomeres from birth, ageing and dying prematurely [29]. While *tert*^{-/-} fish have a lifespan of c.12–20 months, WT fish typically die between 36–42 months of age [29, 30]. In order to study age-related phenotypes in zebrafish, in this study we use an age > 30 months old fish for what we consider old in WT (in the last 25–30% of their lifespan), and we consider the *tert*^{-/-} old fish at the equivalent age (> 12 months) that corresponds to the last 25–30% of their lifespan, approximately, as has been described before [55]. In specific, ‘Old’ was defined as the age at which the majority of the fish present age-associated phenotypes, such as cachexia, loss of body mass and curvature of the spine. These phenotypes develop close to the time of death and are observed at > 30 months of age in WT and at > 12 months in *tert*^{-/-29,30}.

Tissue preparation: paraffin-embedded sections and cryosections

Adult fish were culled by overdose of MS-222, followed by immersion fixation in 4% paraformaldehyde (PFA) buffered at pH 7.0. Whole fish were then processed for paraffin-embedded sections or for cryosections. Importantly, all quantitative comparisons presented in figures were performed in paraffin sections. Cryosections were only used for TCR staining in Fig. 3, since this antibody did not work in paraffin sections, in our hands.

Paraffin-embedded sections

Whole fish were fixed in 4% paraformaldehyde (PFA) buffered at pH 7.0, at 4°C for 48–72 h, decalcified in 0.5 M ethylenediaminetetraacetic acid (EDTA) at pH 8.0 for 48–72 h, and embedded in paraffin by the following series of washes: formalin I (Merck & Co, Kenilworth, NJ, USA) for 10 min, formalin II for 50 min, ethanol 50% for 1 h, ethanol 70% for 1 h, ethanol 95% for 1 h 30 min, ethanol 100% for 2 h, ethanol 100% for 2 h 30 min, 50:50 of ethanol 100%: xilol for 1 h 30 min, xylene I for 3 h, xylene II for 3 h, paraffin I for 3 h and paraffin II for 4 h 30 min. Paraffin-embedded whole fish were then sliced in sagittal 3 μm-thick, using a microtome (Leica RM2265). These sections were then used for immunofluorescence, fluorescence RNA *in situ* hybridisation and Telo-FISH.

Cryopreservation and cryosections

Dissected guts were washed in 1 × phosphate-buffered saline (PBS), cut into anterior, distal and middle portions and were fixed in 4% PFA at 4°C, overnight (ON).

Then, they were washed in cold PBS and immersed in 30% sucrose in PBS, ON at 4°C, for cryopreservation. Individual guts were then embedded in mounting media – optimal cutting temperature compound (OCT, VWR International), snap-frozen in dry ice, and stored at -20°C until cryosectioning. Cryosections were sliced at a 13 µm thickness using a Leica Jung Frigocut cryostat or a Leica CM1860 cryostat. Sections were air dried for 2 h then used for immunohistochemistry or frozen for up to 3 months at -20°C before use.

Immunofluorescence (IF), telomerase (tert) RNA in situ hybridisation (RNA-ISH) and Telomere PNA FISH (Telo-FISH) IF

Before immunofluorescence staining, cryosections were hydrated in PBS at room temperature (RT) for 10 min, and paraffin-embedded sections were deparaffinised and hydrated as follows: histoclear (Scientific Laboratory Supplies, Wilford, Nottingham, UK) 2 × for 5 min, followed by ethanol 100% 2 × for 5 min, ethanol 90% for 5 min, ethanol 70% for 5 min, and distilled water 2 × for 5 min. Antigen retrieval was then performed by sub-boiling simmering in 0.01 M citrate buffer at pH 6.0 for 10 min, using a microwave. After cooling, the sections were permeabilised in PBS 0.5% Triton X-100 for 10 min and blocked in 3% bovine serum albumin (BSA), 5% Goat Serum (or Donkey Serum), 0.3% Tween-20 in PBS, for 1 h. The slides were then incubated with the

primary antibody at 4 °C ON. After washes in PBS 0.1% Tween-20 (3 × 10 min) to remove excess primary antibody, the sections were incubated with secondary antibody at RT for 1 h or at 4°C ON. Slides were then washed as above and incubated in 1 µg/ml of 4',6-diamidino-2-phenylindole (DAPI, Thermo Fisher Scientific) at RT for 10 min. Finally, the slides were washed once in PBS, and mounted with vectashield (Vector Laboratories, Burlingame, CA, USA). The primary and secondary antibody details are described in Tables 1 and 2.

Telomerase (tert) RNA-ISH combined with IF

Telo-FISH or Q-FISH as is sometimes called, was performed on tissues (interphase cells). The Mean Telo-FISH fluorescence signal here shown is a proxy for the relative mean telomere length from all chromosomes in that cell, and each dot does not represent a single telomere, but rather a collection of telomere signal. The signal is proportional to the length of the telomere(s), i.e., the amount of DNA to which the fluorescent probe hybridises to [111].

Paraffin sections were deparaffinised as described, using fresh solutions and bleach-treated glassware to avoid RNase contamination. Where possible, solutions were made up in Diethyl pyrocarbonate (DEPC)-treated H₂O or PBS and autoclaved. Following deparaffinisation, slides were rinsed in DEPC-PBS for 5 min and incubated

Table 1 Primary antibodies used for immunostaining

Antibody, species and type	Dilution factor	Catalogue number; Company, City, Country
PCNA rabbit polyclonal	1:300	GTX124496; GeneTex, Irvine, CA, USA
Rabbit anti-TCR-alpha (N terminus)	1:200	AS-55868, AnaSpec Inc
Mouse anti-RFP	1:500	GTX82561; Genetex
Chicken anti-GFP	1:500	AB13970, Abcam
Rabbit anti L-plastin	1:300	GTX124420, Genetex
Rabbit anti-LC3B	1:200	AB48394, Abcam
Rabbit anti-yH2ax	1:300	GTX127342, Genetex
Rabbit anti-IL-6	1:500	AB6672, Abcam

Table 2 Secondary antibodies used for immunostaining

Antibody, species and type	Dilution factor	Catalogue number; Company, City, Country
Goat anti-rabbit IgG Alexa Fluor [®] 488	1:500	A11008; Invitrogen, Carlsbad, CA, USA
Goat anti-rabbit IgG Alexa Fluor [®] 568	1:500	A11036; Invitrogen, Carlsbad, CA, USA
Donkey anti-rabbit IgG Alexa Fluor [®] 647	1:500	A31573; Thermo Fisher Scientific, Waltham, MA, USA
Goat anti-mouse IgG Alexa Fluor [®] 488	1:500	A11001; Thermo Fisher Scientific, Waltham, MA, USA
Goat anti-mouse IgG Alexa Fluor [®] 568	1:500	10,348,072; Thermo Fisher Scientific, Waltham, MA, USA
Goat anti-mouse IgG Alexa Fluor [®] 647	1:500	A21235; Thermo Fisher Scientific, Waltham, MA, USA

at 37 °C with 200ul of proteinase K at 20ug/ml in DEPC-PBS for 14 min (coverslipped). Slides were rinsed in DEPC-PBS briefly and fixed in 4% PFA for 20 min in a coplin jar. Slides were then rinsed in DEPC-PBS for 10 min at RT and acetylated as follows: 1 ml DEPC- H₂O, 11.2ul Triethanolamine (TEA) and 2.5ul acetic anhydride were made up per slide, immediately mixed and incubated on the slide for 10 min at RT. Slides were then rinsed in DEPC-PBS (10 min × 2) and 1.5 ml prewarmed hybridisation solution ((50% formamide, 2% Blocking Reagent, 0.1% Triton X-100, 0.5% CHAPS, 1 mg/ml yeast RNA, 50ug/ml heparin (sodium salt) (all Sigma Aldrich), 5 mM EDTA and 5xSSC pH7)) was incubated on the slides in a humidified box at 68 °C for 1 h minimum. Prewarmed digoxigenin-labelled probes (see below for probe information) were then added to slides (200ul per slide, at 2-5 ng/ul in hybridisation solution) which were then coverslipped and incubated in a humidified box overnight at 68 °C. Coverslips were removed and slides washed for 1 h at 68 °C in a coplin jar in prewarmed 'solution 1': 25 ml formamide, 12.5 ml 20xSSC pH4.5, 5 ml SDS, 7.5 ml H₂O, followed by 1 h at 68 °C in prewarmed 'solution 2': 25 ml formamide, 5 ml 20xSSCpH4.5, 500ul Tween20, 19.5 ml H₂O. Gentle shaking was used during washes. Slides were rinsed twice with PBS + 0.1% tritonX100 (PB-Triton), twice with maleic acid buffer (100 mM maleic acid, 150 mM NaCl, pH7.5) + 0.1% triton (MABT) then blocked in MABT + 2% Blocking Reagent at RT for 1 h. Anti-DIG-peroxidase (POD) antibody was added at 1:500 in MABT + 2% Blocking reagent, slides were coverslipped and incubated in a humidified box ON at 4 °C. Slides were washed 6 × 20 min in PB-Triton in a coplin jar followed by 2 rinses in 100 mM boric acid pH8.5 + 0.1% triton X-100. Fluorescent tyramides were incubated on the slides at 1:75 in freshly prepared TSA buffer (100 mM Boric acid pH8.5, 0.1% Triton X-100, 2% dextran sulphate, 0.003% H₂O₂, 400ug/ml 4-iodophenol) for 20 min at RT shielded from light. Finally, slides were rinsed 4 × in PB-Triton, and fixed in 4% PFA for 5 min followed by a brief rinse in PBS. After RNA-ISH, immunofluorescence was performed on the same slides, avoiding exposure to light and starting from the permeabilisation step.

tert probe design

Sense and anti-sense DIG-labelled RNA probes were synthesised from 5' and 3' regions of *tert* using DIG RNA Labelling Mix (Roche). A 562 bp 3' region of *tert*, was amplified using primers: *tert* 3' FW, CGG TAT GAC GGC CTA TCA CT and *tert* 3' REV, CAG GTT TTT TTT ACA CCC GC and TA cloned into PCRII (TA Cloning(TM) Kit Dual Promoter, Invitrogen). For antisense probe synthesis, the resulting construct was

linearised with BamHI and transcribed with T7 RNA polymerase (New England Biolabs, (NEB)). For sense probe synthesis, the same plasmid was linearised with ApaI and transcribed with SP6 RNA polymerase (both NEB). 'Full length' *tert* cDNA was amplified using primers FW, ATG TCTGGACAGTACTCGAC and REV, CAGGTTTTT TTTACACCCGC. This was TA cloned as above into PCRII. A 1.5 Kb subregion consisting of the 5' end of this clone up to the first ApaI site was subcloned into PCRII and this 5' *tert* plasmid was then used for probe synthesis of 5' sense and antisense probes. For antisense, this was linearised with HindIII and transcribed with T7. For sense probe, it was linearised with ApaI and transcribed with SP6. A mixture of either 5' and 3' antisense or 5' and 3' sense (control) probes was used on sections in hybridisation buffer so that the final concentration of probe was 2-5 ng/ul.

IF combined with Telo-FISH

The IF protocol was followed as above. After the secondary antibody and PBS 0.1% Tween-20 washes, slides were fixed for 20 min. in 4% PFA, washed three times in PBS and dehydrated with cold 70, 90 and 100% ethanol for 3 min each. After drying for 30 min, sections were denatured for 5 min at 80 °C in hybridisation buffer (70% formamide (Sigma), 2.14 mM MgCl₂, 10 mM Tris pH 7.2, 0.05% blocking reagent (Roche)) containing 0.5 ug/ml Cy-3-labelled telomere specific (CCCTAA) peptide nucleic acid probe (Panagene), followed by hybridization for 2 h at room temperature in the dark. The slides were washed once with 70% formamide in 2xSSC for 10 min, followed by 2 × 10 min washes with 2 × SSC. Sections were incubated with DAPI (SIGMA), mounted and imaged. For Cent-FISH, a custom-made FAM labelled zebrafish specific centromeric probe (based on ZEFRAL1) [60] was added alongside the Cy3-telomeric probe. Sequence of our custom made probe: FAM-OO-tag aca aca ttt cat gca (CRB Discovery- Cambridge Biochemicals).

In vivo assays

Phagocytosis

Delivery of pHrodo™ Green *E. coli* BioParticles™ (Thermo Fisher) to the gut was performed via oral gavage in adult *mpeg⁺-mcherry caax* zebrafish, both at young (c.5 months) and old (c. 35 months) WT ages, and in the absence of telomerase (*tert*^{-/-}) at c.5 months. Zebrafish were not fed for 12/18 h before 5 ml of *E.coli* bioparticles were delivered to zebrafish guts by oral gavage. Fish were sacrificed 4 h post gavage and gut tissue was dissected and processed for cryopreservation and sectioning. Cryosections of zebrafish gut were then imaged for native fluorescence, combined with DAPI nuclear

staining. *mpeg*⁺ cells can be detected by the membrane bound *mcherry caax* and the % of *mpeg*⁺ cells containing visible green E.coli bioparticles inside (were quantified, as a readout for phagocytosis efficiency (the zebrafish gastrointestinal tract is not acidic [62], so the pHRed moiety ensures that these particles increase their fluorescence once phagocytosed into acidic vesicles). We further ensured that the bioparticles were indeed inside the cells by going through all the Z-stacks, of 0.5 mm each.

Gut permeability

Smurf gut permeability was performed as described previously [84], by placing zebrafish (WT and *tert*^{-/-}) of different ages in individual tanks containing 2.5% (w/v) blue #1 [79, 84] in water for 30 min. Individuals were then rinsed under clear water until no more blue colouration could be found in the eluate. Fishes showing extended coloration of blue in their body were considered as Smurfs.

Edu pulse chase

Fish were anaesthetised in 4% tricaine methanesulfonate (MS-222; Covetrus, pharmaceutical grade) after c. 18 h fasting and prepared for Intraperitoneal Injections (IP) of EdU or control solution as follows. Fish were placed in a small bed-like structure made of sponge, located inside a small petri dish and carefully administered 5 ml of 10 mM EdU (Click it EdU Alexa Fluor 647 Imaging Kit (Invitrogen, C10340) or Hanks' Balanced Salt Solution (HBSS) (Gibco, 14,175-053) by IP injection using a 30G 3 ml insulin syringe (BD Micro-Fine U-100 insulin, REF 324,826), following the previously described protocol [112]. Fish were injected once every day for 3 consecutive days at the same times of the day (3-day pulse) and culled on day 4 (1 day chase), for paraffin embedding, sectioning and IF (see Sects. 5.3.1 and 5.4.1). Fish used: WT adult fish of c. 12 months, *tert*^{-/-} "old" 12 months and WT old > 24 months (*N* = 4 for each genotype).

Imaging and quantifications

Paraffin-embedded and cryosections sections were imaged by epifluorescence microscopy, using a Delta-Vision microscope with a 40 × oil objective. In order to quantify the alteration in the staining patterns, a z-projection was generated using ImageJ (Rasband, W.S., ImageJ, U. S. National Institutes of Health, Bethesda, Maryland, USA, <https://imagej.nih.gov/ij/>, 1997–2018.) at least 3 Fields of View (FoV) were imaged, each containing at least two gut villi, per animal. At least three individual animals per genotype were imaged. Raw images were used for quantification and the images were

then processed with Adobe Illustrator 21.0.2 for display purposes.

Calculating the different proportions of immune subtypes within the "hyper-long" telomere population

We used the double transgenic *mhcll:gfp/cd45:dsred* zebrafish line [70] to allow the identification of macrophages/dendritic cells (*mhclldab:gfp⁺cd45:dsred⁺*); B-cells (*mhclldab:gfp⁺cd45:dsred⁻*) and T-cells/neutrophils (*mhclldab:gfp⁻cd45:dsred⁺*) in the zebrafish gut [70] (Fig. 2B). We combined immunofluorescence (IF) staining using anti-GFP and anti-RFP to detect *mhclldab:gfp* and *cd45:dsred* respectively, with telomere PNA-FISH, as described in Sect. 5.4.4 and counterstained with DAPI to identify the nuclei. We then counted all the cells that had differentially "hyper-long" telomeres (very bright red signal as shown in Fig. 1 and 2) and from within those, we counted how many, in percentage, were GFP⁺, DSRED⁺ or double GFP⁺DSRED⁺, i.e., B-cells (*mhclldab:gfp⁺cd45:dsred⁻*), T-cells (*mhclldab:gfp⁻cd45:dsred⁺*) or putative intestinal mononuclear phagocytes (MPs) (Macrophages (MΦs)/dendritics(DCs) (*mhclldab:gfp⁺cd45:dsred⁺*), respectively. We compared and confirmed the results obtained using the *mhcll:gfp/cd45:dsred* transgenic line regarding the percentage of macrophages within the "hyper-long" telomere population by using the *mpeg1.1:mcherry caax*. We combined IF using anti-RFP to detect the *mpeg1.1:mcherry caax*⁺ cell population with the telomere and centromere PNA-FISH as described in Sect. 5.4.4. We then counted the number of "hyper-long" telomere cells (tel/cent ratio above 1.2, as described in Fig. 1) and, from within those, counted how many, in percentage, were *mpeg1.1:mcherry caax*⁺.

Statistical analysis

Statistics were performed using the GraphPad Prism v7.00. Normality was assessed by the Shapiro–Wilk test. For normally distributed data where most of the groups had a sample size of ≥ 5 unpaired t-test was used to compare 2 data points. For non-normally distributed data and/or data containing less than 5 animals in most of the groups Mann–Whitney test and Kruskal–Wallis tests were used instead. Chi-square was performed on the comparison between the number of Smurfs versus non-Smurfs in the intestinal permeability assay. A critical value for significance of *p* < 0.05 was used throughout all analysis. There were no repeated measurements performed in this study. Quantifications were either performed blind or/and by different individuals to increase robustness and confidence in the results obtained.

Supplementary Information

The online version contains supplementary material available at <https://doi.org/10.1186/s12979-022-00287-8>.

Additional file 1: Supplementary Figure 1. Telomere length decreases in gut immune cells with ageing. **A)** Quantification of the relative telomere length of L-plastin+ cells, from gut paraffin sections, using combined immunostaining for anti-L-plastin and telomere in situ hybridization (Telo-FISH), together with the near-centromeric probe (Cent-FISH), as in Figure 1. **B)** From the same quantifications as in A), we can calculate the % of gut L-plastin+ cells with “hyper-long” telomeres. Young animals are c.5 months old and old animals are >30-36 months old.

Additional file 2: Supplementary Figure 2. Immune cells in the gut retain longer telomeres than epithelial cells, despite telomere shortening over time. **A)** Quantification of the relative telomere length of L-plastin+ cells, from gut paraffin sections, using combine immunostaining for anti-L-plastin and telomere in situ hybridization (Telo-FISH), together with the near-centromeric probe (Cent-FISH), as in Figure 1. Young animals are c.5 months old and old animals are >30-36 months old. **B)** EdU pulse-chase experiment schematics, where fish were injected with EdU by IP for 3 consecutive days to label all proliferating cells. Gut tissue was collected on day 4 (1-day post-chase) and **B1)** the % of EdU+ L-plastin+ cells was quantified and averaged per animal per genotype.

Acknowledgements

We thank Dr. Valery Wittamer for kindly sharing the *mhcll:gfp/cd45:dred* zebrafish transgenic line and Dr. Simon Johnston for sharing the *tnfa:GFP* crossed with the *mpeg1.1:mcherry caax* line, so that we could cross it back into the *tert*^{-/-} line. We also thank Dr. Simon Johnston and Dr. Daniel Humphreys for critical reading of the manuscript. We thank Prof. Ilaria Bellantuono for useful discussions during development of this work. We thank Dr. Miguel Godinho Ferreira for support during CMH's post-doc, in which the work we did and publish together^{55,56} provided key insights that preceded the development of this work. We also thank Dr. Miguel Godinho Ferreira for sharing the *tert*^{-/-} line from the same outcross that had been used in the previous aforementioned studies. Finally, we thank the University of Sheffield Aquarium team for excellent care of our animals as well as the Wolfson Microscopy Facility for outstanding support.

Authors' contributions

PSE, RM, ET, AF and CMH have performed experiments and analysed data. SAR has provided key zebrafish lines of different ages and has helped design and analyse data. CMH prepared all the figures and wrote the manuscript with input from co-authors. The author(s) read and approved the final manuscript.

Funding

CMH was funded by a Sheffield University Vice Chancellor's Research Fellowship and a Sir. Henry Dale Fellowship by the Wellcome Trust and Royal Society. This research was funded in whole, or in part, by the Wellcome Trust [UNS35121]. For the purpose of Open Access, the author has applied a CC BY public copyright licence to any Author Accepted Manuscript version arising from this submission.

PSE was funded by a PDRA salary included in CMH Sir. Henry Dale Fellowship (The Wellcome Trust and Royal Society).

RRM was funded by a University of Sheffield, UK PhD studentship.

EJT was an internship student by Sheffield Hallam University.

AF was a BMS internship student by the University of Sheffield.

SAR was funded by the Medical Research Council (MRC), UK.

Availability of data and materials

The datasets and source data generated during and/or analysed during the current study are available from the corresponding author on reasonable request.

Declarations

Competing interests

The authors declare no competing interests.

Author details

¹The Bateson Centre, MRC-Arthritis Research UK Centre for Integrated Research Into Musculoskeletal Ageing and Department of Oncology and Metabolism, Healthy Lifespan Institute, University of Sheffield Medical School, Sheffield, UK. ²The Bateson Centre and Department of Infection, Immunity and Cardiovascular Disease, Medical School, University of Sheffield, Sheffield, UK.

Received: 11 February 2022 Accepted: 17 June 2022

Published online: 11 July 2022

References

- de Lange T. Shelterin: the protein complex that shapes and safeguards human telomeres. *Genes Dev.* 2005;19:2100–10. <https://doi.org/10.1101/gad.1346005>.
- Levy MZ, Allsopp RC, Futcher AB, Greider CW, Harley CB. Telomere end-replication problem and cell aging. *J Mol Biol.* 1992;225:951–60. [https://doi.org/10.1016/0022-2836\(92\)90096-3](https://doi.org/10.1016/0022-2836(92)90096-3).
- Bodnar AG. Extension of Life-Span by Introduction of Telomerase into Normal Human Cells. *Science.* 1998;279:349–52. <https://doi.org/10.1126/science.279.5349.349>.
- d'Adda di Fagagna F, et al. A DNA damage checkpoint response in telomere-initiated senescence. *Nature.* 2003;426(6963):194–8. <https://doi.org/10.1038/nature02118>.
- Ferreira MG, Miller KM, Cooper JP. Indecent exposure: when telomeres become uncapped. *Mol Cell.* 2004;13:7–18.
- Shay JW, Wright WE. Hallmarks of telomeres in ageing research. *J Pathol.* 2007;211:114–23. <https://doi.org/10.1002/path.2090>.
- López-Otin C, Blasco MA, Partridge L, Serrano M, Kroemer G. The hallmarks of aging. *Cell.* 2013;153(6):1194–217. <https://doi.org/10.1016/j.cell.2013.05.039>.
- Dimri GP, et al. A biomarker that identifies senescent human cells in culture and in aging skin in vivo. *Proc Natl Acad Sci USA.* 1995;92:9363–7.
- Ovadya Y, Krizhanovsky V. Senescent cells: SASPected drivers of age-related pathologies. *Biogerontology.* 2014;15:627–42. <https://doi.org/10.1007/s10522-014-9529-9>.
- Forsyth NR, Wright WE, Shay JW. Telomerase and differentiation in multicellular organisms: turn it off, turn it on, and turn it off again. *Differentiation.* 2002;69:188–97. <https://doi.org/10.1046/j.1432-0436.2002.690412.x>.
- Flores I, et al. The longest telomeres: a general signature of adult stem cell compartments. *Genes Dev.* 2008;22:654–67. <https://doi.org/10.1101/gad.451008>.
- Hodes RJ, Hathcock KS, Weng NP. Telomeres in T and B cells. *Nat Rev Immunol.* 2002;2:699–706. <https://doi.org/10.1038/nri890>.
- Henson SM, Akbar AN. Memory T-cell homeostasis and senescence during aging. *Adv Exp Med Biol.* 2010;684:189–97.
- Akbar AN, Vukmanovic-Stejic M. Telomerase in T lymphocytes: use it and lose it? *J Immunol.* 2007;178:6689–94.
- Reed JR, et al. Telomere erosion in memory T cells induced by telomerase inhibition at the site of antigenic challenge in vivo. *J Exp Med.* 2004;199:1433–43. <https://doi.org/10.1084/jem.20040178>.
- Lobetti-Bodoni C, Bernocco E, Genuardi E, Boccadoro M, Ladetto M. Telomeres and telomerase in normal and malignant B-cells. *Hematol Oncol.* 2010;28:157–67. <https://doi.org/10.1002/hon.937>.
- Harley CB, et al. Telomerase, cell immortality, and cancer. *Cold Spring Harb Symp Quant Biol.* 1994;59:307–15. <https://doi.org/10.1101/SQB.1994.059.01.035>.
- Findeisen HM, et al. Telomerase deficiency in bone marrow-derived cells attenuates angiotensin II-induced abdominal aortic aneurysm formation. *Arterioscler Thromb Vasc Biol.* 2011;31:253–60. <https://doi.org/10.1161/ATVBAHA.110.218545>.
- Gizard F, et al. Telomerase activation in atherosclerosis and induction of telomerase reverse transcriptase expression by inflammatory stimuli in macrophages. *Arterioscler Thromb Vasc Biol.* 2011;31:245–52. <https://doi.org/10.1161/ATVBAHA.110.219808>.
- Narducci ML, et al. High telomerase activity in neutrophils from unstable coronary plaques. *J Am Coll Cardiol.* 2007;50:2369–74. <https://doi.org/10.1016/j.jacc.2007.08.048>.

21. Segal-Bendirdjian E, Geli V. Non-canonical roles of telomerase: unravelling the imbroglgio. *Front Cell Dev Biol.* 2019;7:332. <https://doi.org/10.3389/fcell.2019.00332>.
22. Zhou J, Ding D, Wang M, Cong YS. Telomerase reverse transcriptase in the regulation of gene expression. *BMB Rep.* 2014;47:8–14.
23. Park JI, et al. Telomerase modulates Wnt signalling by association with target gene chromatin. *Nature.* 2009;460:66–72. <https://doi.org/10.1038/nature08137>.
24. Cao X, et al. The use of transformed IMR90 cell model to identify the potential extra-telomeric effects of hTERT in cell migration and DNA damage response. *BMC Biochem.* 2014;15:17. <https://doi.org/10.1186/1471-2091-15-17>.
25. Parkinson EK, Fitchett C, Cereser B. Dissecting the non-canonical functions of telomerase. *Cytogenet Genome Res.* 2008;122:273–80. <https://doi.org/10.1159/000167813>.
26. Choi J, et al. TERT promotes epithelial proliferation through transcriptional control of a Myc- and Wnt-related developmental program. *PLoS Genet.* 2008;4: e10. <https://doi.org/10.1371/journal.pgen.0040010>.
27. Qu Y, et al. Enhanced migration and CXCR4 over-expression in fibroblasts with telomerase reconstitution. *Mol Cell Biochem.* 2008;313:45–52. <https://doi.org/10.1007/s11010-008-9740-6>.
28. Sato N, et al. Telomerase activity of cultured human pancreatic carcinoma cell lines correlates with their potential for migration and invasion. *Cancer.* 2001;91:496–504.
29. Kushner EJ, et al. Human aging and CD31+ T-cell number, migration, apoptotic susceptibility, and telomere length. *J Appl Physiol.* 2010;108(109):1756–61. <https://doi.org/10.1152/jappphysiol.00601.2010>.
30. Yu L, et al. hTERT promoter activity identifies osteosarcoma cells with increased EMT characteristics. *Oncol Lett.* 2014;7:239–44. <https://doi.org/10.3892/ol.2013.1692>.
31. Chen PC, et al. Overexpression of human telomerase reverse transcriptase promotes the motility and invasiveness of HepG2 cells in vitro. *Oncol Rep.* 2013;30:1157–64. <https://doi.org/10.3892/or.2013.2563>.
32. Deacon K, Knox AJ. PINX1 and TERT are required for TNF-alpha-induced airway smooth muscle chemokine gene expression. *J Immunol.* 2018;200:1283–94. <https://doi.org/10.4049/jimmunol.1700414>.
33. Ghosh A, et al. Telomerase directly regulates NF-kappaB-dependent transcription. *Nat Cell Biol.* 2012;14:1270–81. <https://doi.org/10.1038/ncb2621>.
34. Mattiussi M, Tilman G, Lenglez S, Decottignies A. Human telomerase represses ROS-dependent cellular responses to Tumor Necrosis Factor-alpha without affecting NF-kB activation. *Cell Signal.* 2012;24:708–17. <https://doi.org/10.1016/j.cellsig.2011.11.004>.
35. Sarin KY, et al. Conditional telomerase induction causes proliferation of hair follicle stem cells. *Nature.* 2005;436:1048–52. <https://doi.org/10.1038/nature03836>.
36. Cao Y, Li H, Deb S, Liu JP. TERT regulates cell survival independent of telomerase enzymatic activity. *Oncogene.* 2002;21:3130–8. <https://doi.org/10.1038/sj.onc.1205419>.
37. Rahman R, Latonen L, Wiman KG. hTERT antagonizes p53-induced apoptosis independently of telomerase activity. *Oncogene.* 2005;24:1320–7. <https://doi.org/10.1038/sj.onc.1208232>.
38. Ahmed S, et al. Telomerase does not counteract telomere shortening but protects mitochondrial function under oxidative stress. *J Cell Sci.* 2008;121:1046–53. <https://doi.org/10.1242/jcs.019372>.
39. Haendeler J, et al. Mitochondrial telomerase reverse transcriptase binds to and protects mitochondrial DNA and function from damage. *Arterioscler Thromb Vasc Biol.* 2009;29:929–35. <https://doi.org/10.1161/ATVBAHA.109.185546>.
40. Bain CC, Mowat AM. Intestinal macrophages - specialised adaptation to a unique environment. *Eur J Immunol.* 2011;41:2494–8. <https://doi.org/10.1002/eji.201141714>.
41. Chassaing B, Kumar M, Baker MT, Singh V, Vijay-Kumar M. Mammalian gut immunity. *Biomed J.* 2014;37:246–58. <https://doi.org/10.4103/2319-4170.130922>.
42. Bain CC, Mowat AM. Macrophages in intestinal homeostasis and inflammation. *Immunol Rev.* 2014;260:102–17. <https://doi.org/10.1111/imr.12192>.
43. Larabi A, Barnich N, Nguyen HTT. New insights into the interplay between autophagy, gut microbiota and inflammatory responses in IBD. *Autophagy.* 2020;16:38–51. <https://doi.org/10.1080/15548627.2019.1635384>.
44. Boyapati RK, Rossi AG, Satsangi J, Ho GT. Gut mucosal DAMPs in IBD: from mechanisms to therapeutic implications. *Mucosal Immunol.* 2016;9:567–82. <https://doi.org/10.1038/mi.2016.14>.
45. Moss C, Dhillon WS, Frost G, Hickson M. Gastrointestinal hormones: the regulation of appetite and the anorexia of ageing. *J Hum Nutr Diet.* 2012;25:3–15. <https://doi.org/10.1111/j.1365-277X.2011.01211.x>.
46. Bhutto A, Morley JE. The clinical significance of gastrointestinal changes with aging. *Curr Opin Clin Nutr Metab Care.* 2008;11:651–60. <https://doi.org/10.1097/MCO.0b013e32830b5d37>.
47. Britton E, McLaughlin JT. Ageing and the gut. *Proc Nutr Soc.* 2013;72:173–7. <https://doi.org/10.1017/S0029665112002807>.
48. Marjoram L, et al. Epigenetic control of intestinal barrier function and inflammation in zebrafish. *Proc Natl Acad Sci USA.* 2015;112:2770–5. <https://doi.org/10.1073/pnas.1424089112>.
49. Malnutrition among Older People in the Community: Policy Recommendations for Change. (European Nutrition for Health Alliance, 2006). <https://www.bapen.org.uk/resources-and-education/publications-and-reports/other-reports/malnutrition-among-older-people-in-the-community>.
50. Roberts SB, et al. Control of food intake in older men. *JAMA.* 1994;272:1601–6. <https://doi.org/10.1001/jama.1994.03520200057036>.
51. de Jong PR, Gonzalez-Navajas JM, Jansen NJ. The digestive tract as the origin of systemic inflammation. *Crit Care.* 2016;20:279. <https://doi.org/10.1186/s13054-016-1458-3>.
52. Rera M, Azizi MJ, Walker DW. Organ-specific mediation of lifespan extension: more than a gut feeling? *Ageing Res Rev.* 2013;12:436–44. <https://doi.org/10.1016/j.arr.2012.05.003>.
53. Cardoso Ba, Biological and therapeutic implications, et al. Aberrant signaling in T-cell acute lymphoblastic leukemia. *Braz J Med Biol Res.* 2008;41:344–50. <https://doi.org/10.1590/S0100-879X2008005000016>.
54. El Mai M, Guignon JM, Pourchet T, Kang D, Yue JX, Ferreira MG. Telomere elongation in the gut extends zebrafish lifespan. *bioRxiv* 2022.01.10.475664. <https://doi.org/10.1101/2022.01.10.475664>.
55. Carneiro MC, et al. short telomeres in key tissues initiate local and systemic aging in zebrafish. *PLoS Genet.* 2016;12: e1005798. <https://doi.org/10.1371/journal.pgen.1005798>.
56. Henriques CM, Carneiro MC, Tenente IM, Jacinto A, Ferreira MG. Telomerase is required for zebrafish lifespan. *PLoS Genet.* 2013;9: e1003214. <https://doi.org/10.1371/journal.pgen.1003214>.
57. Anachelin M, et al. Premature aging in telomerase-deficient zebrafish. *Dis Model Mech.* 2013;6:1101–12. <https://doi.org/10.1242/dmm.011635>.
58. Anachelin M, et al. Premature aging in telomerase-deficient zebrafish. *Dis Model Mech.* 2013;6:1101–12. <https://doi.org/10.1242/dmm.011635>.
59. Franceschi C, Campisi J. Chronic inflammation (inflammaging) and its potential contribution to age-associated diseases. *J Gerontol A Biol Sci Med Sci.* 2014;69(Suppl 1):S4–9. <https://doi.org/10.1093/gerona/glu057>.
60. Phillips RB, Reed KM. Localization of repetitive DNAs to zebrafish (*Danio rerio*) chromosomes by fluorescence in situ hybridization (FISH). *Chromosome Res.* 2000;8(1):27–35. <https://doi.org/10.1023/a:1009271017998>.
61. Martins RR, Ellis PS, MacDonald RB, Richardson RJ, Henriques CM. Resident immunity in tissue repair and maintenance: the zebrafish model coming of age. *Front Cell Dev Biol.* 2019;7:12. <https://doi.org/10.3389/fcell.2019.00012>.
62. Brugman S. The zebrafish as a model to study intestinal inflammation. *Dev Comp Immunol.* 2016;64:82–92. <https://doi.org/10.1016/j.dci.2016.02.020>.
63. Wang Z, et al. Morphological and molecular evidence for functional organization along the rostrocaudal axis of the adult zebrafish intestine. *BMC Genomics.* 2010;11:392. <https://doi.org/10.1186/1471-2164-11-392>.
64. Davidson AJ, Zon LI. The “definitive” (and “primitive”) guide to zebrafish hematopoiesis. *Oncogene.* 2004;23:7233–46. <https://doi.org/10.1038/sj.onc.1207943>.
65. Dee CT, et al. CD4-transgenic zebrafish reveal tissue-resident Th2- and regulatory T cell-like populations and diverse mononuclear phagocytes.

- J Immunol. 2016;197:3520–30. <https://doi.org/10.4049/jimmunol.1600959>.
66. Brugman S, Witte M, Scholman RC, Klein MR, Boes M, Nieuwenhuis EE. T lymphocyte-dependent and -independent regulation of Cxcl8 expression in zebrafish intestines. *J Immunol*. 2014;192(1):484–91. <https://doi.org/10.4049/jimmunol.1301865>.
 67. Brugman S, et al. T lymphocytes control microbial composition by regulating the abundance of *Vibrio* in the zebrafish gut. *Gut Microbes*. 2014;5:737–47. <https://doi.org/10.4161/19490976.2014.972228>.
 68. Bojarczuk A, et al. Cryptococcus neoformans Intracellular Proliferation and Capsule Size Determines Early Macrophage Control of Infection. *Sci Rep*. 2016;6:21489. <https://doi.org/10.1038/srep21489>.
 69. Renshaw SA, et al. A transgenic zebrafish model of neutrophilic inflammation. *Blood*. 2006;108:3976–8. <https://doi.org/10.1182/blood-2006-05-024075>.
 70. Wittamer V, Bertram JY, Gutschow PW, Traver D. Characterization of the mononuclear phagocyte system in zebrafish. *Blood*. 2011;117:7126–35. <https://doi.org/10.1182/blood-2010-11-321448>.
 71. Ferrero G, et al. The macrophage-expressed gene (mpeg) 1 identifies a subpopulation of B cells in the adult zebrafish. *J Leukoc Biol*. 2020;107:431–43. <https://doi.org/10.1002/JLB.1A1119-223R>.
 72. Ellis PS, Martins RR, Thompson EJ, Farhat A, Renshaw SA, Henriques CM. A subset of gut leukocytes have telomerase-dependent "hyper-long" telomeres and require telomerase for function in zebrafish. *bioRxiv*. 2022.01.31.478480. <https://doi.org/10.1101/2022.01.31.478480>.
 73. Roh JJ, et al. Hexokinase 2 is a molecular bridge linking telomerase and autophagy. *PLoS ONE*. 2018;13:e0193182. <https://doi.org/10.1371/journal.pone.0193182>.
 74. Hughes WE, et al. critical interaction between telomerase and autophagy in mediating flow-induced human arteriolar vasodilation. *Arterioscler Thromb Vasc Biol*. 2021;41:446–57. <https://doi.org/10.1161/ATVBAHA.120.314944>.
 75. Song H, et al. HIF-1 α -mediated telomerase reverse transcriptase activation inducing autophagy through mammalian target of rapamycin promotes papillary thyroid carcinoma progression during hypoxia stress. *Thyroid*. 2021;31:233–46. <https://doi.org/10.1089/thy.2020.0023>.
 76. Ding X, et al. The regulation of ROS- and BECN1-mediated autophagy by human telomerase reverse transcriptase in glioblastoma. *Oxid Med Cell Longev*. 2021;2021:6636510. <https://doi.org/10.1155/2021/6636510>.
 77. Fernando MR, Reyes JL, Iannuzzi J, Leung G, McKay DM. The pro-inflammatory cytokine, interleukin-6, enhances the polarization of alternatively activated macrophages. *PLoS ONE*. 2014;9: e94188. <https://doi.org/10.1371/journal.pone.0094188>.
 78. Agius E, et al. Decreased TNF- α synthesis by macrophages restricts cutaneous immunosurveillance by memory CD4⁺ T cells during aging. *J Exp Med*. 2009;206:1929–40. <https://doi.org/10.1084/jem.20090896>.
 79. Martins RR, McCracken AW, Simons MJ, Henriques CM, Rera M. How to Catch a Smurf? - Ageing and Beyond... In vivo Assessment of Intestinal Permeability in Multiple Model Organisms. *Bio Protoc*. 2018;8(3):e2722. <https://doi.org/10.21769/BioProtoc.2722>.
 80. Ma TY, et al. TNF- α -induced increase in intestinal epithelial tight junction permeability requires NF- κ B activation. *Am J Physiol Gastrointest Liver Physiol*. 2004;286:G367–376. <https://doi.org/10.1152/ajpgi.00173.2003>.
 81. Pender SL, Quinn JJ, Sanderson IR, MacDonald TT. Butyrate upregulates stromelysin-1 production by intestinal mesenchymal cells. *Am J Physiol Gastrointest Liver Physiol*. 2000;279:G918–924. <https://doi.org/10.1152/ajpgi.2000.279.5.G918>.
 82. Nouri M, Bredberg A, Westrom B, Lavasani S. Intestinal barrier dysfunction develops at the onset of experimental autoimmune encephalomyelitis, and can be induced by adoptive transfer of auto-reactive T cells. *PLoS ONE*. 2014;9: e106335. <https://doi.org/10.1371/journal.pone.0106335>.
 83. Tricoire H, Rera M. A new, discontinuous 2 phases of aging model: lessons from *drosophila melanogaster*. *PLoS ONE*. 2015;10: e0141920. <https://doi.org/10.1371/journal.pone.0141920>.
 84. Dambrose E, et al. Two phases of aging separated by the Smurf transition as a public path to death. *Sci Rep*. 2016;6:23523. <https://doi.org/10.1038/srep23523>.
 85. Lee HW, et al. Essential role of mouse telomerase in highly proliferative organs. *Nature*. 1998;392:569–74. <https://doi.org/10.1038/333345>.
 86. Henriques CM, Ferreira MG. Consequences of telomere shortening during lifespan. *Curr Opin Cell Biol*. 2012;24:804–8. <https://doi.org/10.1016/j.ceb.2012.09.007>.
 87. Henson SM, Macaulay R, Franzese O, Akbar AN. Reversal of functional defects in highly differentiated young and old CD8 T cells by PDL blockade. *Immunology*. 2012;135:355–63. <https://doi.org/10.1111/j.1365-2567.2011.03550.x>.
 88. Barnes RP, Fouquerel E, Oprea PL. The impact of oxidative DNA damage and stress on telomere homeostasis. *Mech Ageing Dev*. 2019;177:37–45. <https://doi.org/10.1016/j.mad.2018.03.013>.
 89. Kang Y, et al. Telomere dysfunction disturbs macrophage mitochondrial metabolism and the NLRP3 inflammasome through the PGC-1 α /TNFAIP3 axis. *Cell Rep*. 2018;22:3493–506. <https://doi.org/10.1016/j.celrep.2018.02.071>.
 90. Bain CC, Bravo-Blas A, Scott CL, et al. Constant replenishment from circulating monocytes maintains the macrophage pool in the intestine of adult mice [published correction appears in *Nat Immunol*. 2014 Nov;15(11):1090]. *Nat Immunol*. 2014;15(10):929–37. <https://doi.org/10.1038/ni.2967>.
 91. Alcaraz-Pérez F, et al. A non-canonical function of telomerase RNA in the regulation of developmental myelopoiesis in zebrafish. *Nat Commun*. 2014;5:3228. <https://doi.org/10.1038/ncomms4228>.
 92. Martínez-Balsalobre E, Anchelín-Flageul M, Alcaraz-Pérez F, García-Castillo J, Hernández-Silva D, Mione MC, Mulero V, Cayuela ML. Telomerase and Alternative Lengthening of Telomeres coexist in the regenerating zebrafish caudal fins. *bioRxiv* 2021.11.15.468592. <https://doi.org/10.1101/2021.11.15.468592>.
 93. Shwartz A, Goessling W, Yin C. Macrophages in zebrafish models of liver diseases. *Front Immunol*. 2019;10:2840. <https://doi.org/10.3389/fimmu.2019.02840>.
 94. Gursel I, et al. Repetitive elements in mammalian telomeres suppress bacterial DNA-induced immune activation. *J Immunol*. 2003;171:1393–400.
 95. Yazar V, et al. A suppressive oligodeoxynucleotide expressing TTAGGG motifs modulates cellular energetics through the mTOR signaling pathway. *Int Immunol*. 2020;32:39–48. <https://doi.org/10.1093/intimm/dxz059>.
 96. Wu MY, Lu JH. Autophagy and Macrophage Functions: Inflammatory Response and Phagocytosis. *Cells*. 2019;9(1):70. Published 2019 Dec 27. <https://doi.org/10.3390/cells9010070>.
 97. Pearce EL, Pearce EJ. Metabolic pathways in immune cell activation and quiescence. *Immunity*. 2013;38:633–43. <https://doi.org/10.1016/j.immuni.2013.04.005>.
 98. Martínez J, et al. Molecular characterization of LC3-associated phagocytosis reveals distinct roles for Rubicon, NOX2 and autophagy proteins. *Nat Cell Biol*. 2015;17:893–906. <https://doi.org/10.1038/ncb3192>.
 99. Balla KM, et al. Eosinophils in the zebrafish: prospective isolation, characterization, and eosinophilia induction by helminth determinants. *Blood*. 2010;116:3944–54. <https://doi.org/10.1182/blood-2010-03-267419>.
 100. Fagiolo U, et al. Increased cytokine production by peripheral blood mononuclear cells from healthy elderly people. *Ann NY Acad Sci*. 1992;663:490–3. <https://doi.org/10.1111/j.1749-6632.1992.tb38712.x>.
 101. Bruunsgaard H, Andersen-Ranberg K, Hjelmberg J, Pedersen BK, Jeune B. Elevated levels of tumor necrosis factor α and mortality in centenarians. *Am J Med*. 2003;115:278–83. [https://doi.org/10.1016/s0002-9343\(03\)00329-2](https://doi.org/10.1016/s0002-9343(03)00329-2).
 102. Thevaranjan N, et al. Age-associated microbial dysbiosis promotes intestinal permeability, systemic inflammation, and macrophage dysfunction. *Cell Host Microbe*. 2018;23:570. <https://doi.org/10.1016/j.chom.2018.03.006>.
 103. Suzuki T, Yoshinaga N, Tanabe S. Interleukin-6 (IL-6) regulates claudin-2 expression and tight junction permeability in intestinal epithelium. *J Biol Chem*. 2011;286:31263–71. <https://doi.org/10.1074/jbc.M111.238147>.
 104. Kale A, Sharma A, Stolzing A, Desprez PY, Campisi J. Role of immune cells in the removal of deleterious senescent cells. *Immun Ageing*. 2020;17:16. <https://doi.org/10.1186/s12979-020-00187-9>.

105. Yun MH, Davaapil H, Brockes JP. Recurrent turnover of senescent cells during regeneration of a complex structure. *Elife*. 2015;4:e05505. Published 2015 May 5. <https://doi.org/10.7554/eLife.05505>.
106. da Silva PFL, et al. The bystander effect contributes to the accumulation of senescent cells in vivo. *Aging Cell*. 2019;18: e12848. <https://doi.org/10.1111/accel.12848>.
107. Acosta JC, et al. A complex secretory program orchestrated by the inflammasome controls paracrine senescence. *Nat Cell Biol*. 2013;15:978–90. <https://doi.org/10.1038/ncb2784>.
108. Sharma R. Emerging interrelationship between the gut microbiome and cellular senescence in the context of aging and disease: perspectives and therapeutic opportunities. *Probiotics Antimicrob Proteins*. 2022. <https://doi.org/10.1007/s12602-021-09903-3>.
109. Nagpal R, et al. Gut microbiome and aging: Physiological and mechanistic insights. *Nutr Healthy Aging*. 2018;4:267–85. <https://doi.org/10.3233/NHA-170030>.
110. Tan Y, et al. Save your gut save your age: The role of the microbiome in stem cell ageing. *J Cell Mol Med*. 2019;23:4866–75. <https://doi.org/10.1111/jcmm.14373>.
111. Lai TP, Wright WE, Shay JW. Comparison of telomere length measurement methods. *Philos Trans R Soc Lond B Biol Sci*. 2018;373(1741):20160451. <https://doi.org/10.1098/rstb.2016.0451>.
112. Kinkel MD, Eames SC, Philipson LH, Prince VE. Intraperitoneal injection into adult zebrafish. *J Vis Exp*. 2010. <https://doi.org/10.3791/2126>.

Publisher's Note

Springer Nature remains neutral with regard to jurisdictional claims in published maps and institutional affiliations.

Ready to submit your research? Choose BMC and benefit from:

- fast, convenient online submission
- thorough peer review by experienced researchers in your field
- rapid publication on acceptance
- support for research data, including large and complex data types
- gold Open Access which fosters wider collaboration and increased citations
- maximum visibility for your research: over 100M website views per year

At BMC, research is always in progress.

Learn more biomedcentral.com/submissions

